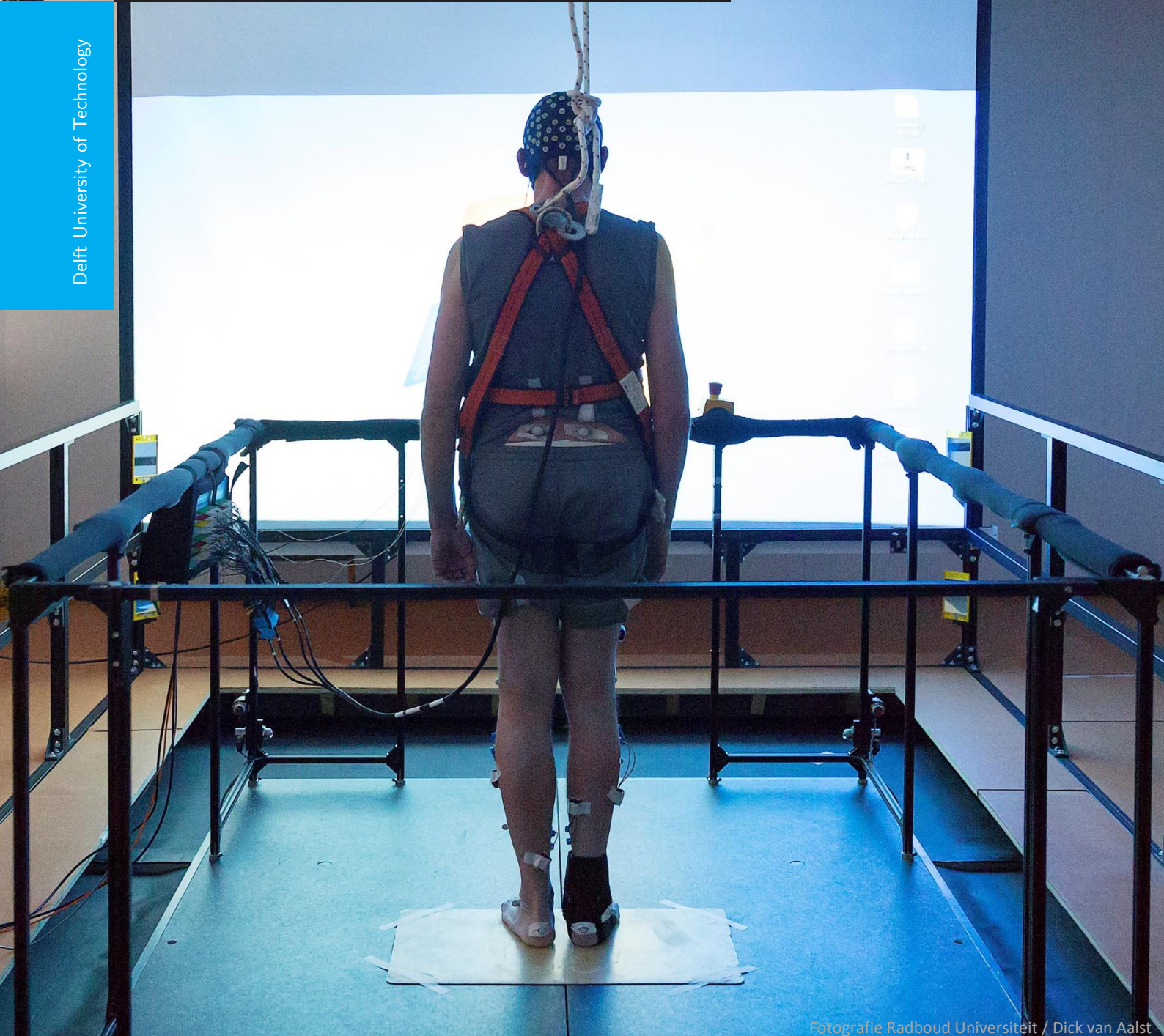


Cortical activity during preparation and inhibition of responses to balance perturbations

J. van der Cruisen

Delft University of Technology



Fotografie Radboud Universiteit / Dick van Aalst

CORTICAL ACTIVITY DURING PREPARATION AND INHIBITION OF RESPONSES TO BALANCE PERTURBATIONS

by

J. van der Cruijssen

in partial fulfillment of the requirements for the degree of

Master of Science
in Biomedical Engineering

at the Delft University of Technology,
to be defended publicly on Friday January 29, 2016 at 10:30 AM.

Student number: 4076729
Project duration: June 24, 2015 – January 29, 2016
Supervisor: dr. ir. A. C. Schouten
Thesis committee: dr. T. Solis-Escalante, TU Delft
dr. ir. J. W. van Wingerden, TU Delft
dr. V. Weerdesteyn, Radboud University Medical Centre, Nijmegen

An electronic version of this thesis is available at <http://repository.tudelft.nl/>.

CONTENTS

Glossary	1
Summary	3
1 Introduction	5
1.1 Background	5
1.2 Problem statement	5
1.3 Goal	6
1.4 Approach	6
1.5 Hypothesis	6
2 Methods	7
2.1 Participants	7
2.2 Platform	7
2.3 Experimental protocol	7
2.3.1 Instructions	8
2.4 Data acquisition	9
2.5 Data Preprocessing	9
2.6 Platform performance	9
2.7 Data analysis	10
2.7.1 Source identification and localisation	10
2.7.2 Component Analysis	11
2.7.3 Head-motion	11
3 Results	13
3.1 Data preprocessing	13
3.2 Platform	13
3.2.1 Clustering	14
3.2.2 Time-domain	14
3.2.3 Time-frequency domain	15
3.3 Head motion	16
4 Discussion	19
4.1 Data quality	19
4.1.1 Artefacts	19
4.1.2 ICA	19
4.2 Time-domain	20
4.3 Time-frequency domain	21
4.4 Recommendations	22
5 Conclusion	23
Bibliography	25
A Head Motion plots	29
B CVA Pilot	33
B.1 Results	33
C Matlab code	37
C.1 Preprocessing	37
C.2 Study analysis	47

GLOSSARY

AMICA	Adaptive Mixture Independent Component Analysis.
CMO	Committee for human research; commissie voor Mensgebonden Onderzoek.
CNV	contingent negative variation.
CVA	Cerebrovascular accident.
EEG	Electroencephalography.
EMG	Electromyography.
EOG	Electrooculography.
ERD	Event-related desynchronisation.
ERP	Event-related potential.
ERS	Event-related synchronisation.
ERSP	Event-related spectral perturbations.
fNIRS	functional near-infrared spectroscopy.
Frequency bands	
δ	0 – 4 Hz.
θ	5 – 7 Hz.
α	8 – 15 Hz.
β	16 – 30 Hz.
γ	31 – 50 Hz.
ICA	Independent Component Analysis.
PD	Parkinson's disease.
RE	Rejected epochs.
RFS	Radboud Falls Simulator.
RV	Residual variance.
SD	standard deviation.

SUMMARY

Yearly, over 400,000 fatal falls occur. People older than 65 years, and especially people suffering from neurological diseases, are at highest risk. To better understand why these groups are at higher risk, the involvement of the cortex has been subject of neurological research. Mobile neuroimaging methods such as functional near-infrared spectroscopy (fNIRS) and electroencephalography (EEG) have been used to study balance control during real-time balance tasks. Research so far has shown involvement of the prefrontal, premotor, motor and parietal cortices of both hemispheres in balance tasks. Recent studies have concentrated on what happens just before balance is lost and what happens when a compensative step is made. The latter is, however, not always possible due to environmental or physical constraints. If a compensative step is inhibited for too long, a fall may result. The goal of this current study is to investigate differences in cortical activity when recovery from a balance perturbation is done by taking a compensatory step or when the step is inhibited and a different strategy is used. It is expected that neural sources around the central region of the head show phase synchronisation in the frequency ranges from 5 to 8 Hz and from 16 to 30 Hz. Phase desynchronisation is expected to occur at the frequency range from 9 to 15 Hz. Furthermore, it is hypothesised that modulation is at a higher magnitude in the condition where participants are instructed to inhibit their step.

A balance experiment is set up in which 10 healthy adults receive 100 perturbations by quickly accelerating the platform on which they stand, while neural activity is recorded using a high-density EEG cap. The platform used in this study can accelerate up to 4.5 ms^{-2} in any direction of the transverse plane. In 50 trials, participants receive a visual instruction that instructs them that they are allowed to respond to the perturbation by taking a step. In the other 50 trials, the instruction given is to keep their feet in place. All trials are at the same perturbation magnitude, which varies among participants. The perturbation magnitude is at the maximum platform acceleration participants can withstand without taking a step. One of the main challenges arising are artefacts on the EEG data introduced by muscular activity and head motion. These artefacts are larger in magnitude than cortical signals and have overlapping frequencies. Although participants receive instructions on how to minimize artefacts from arising, it is not possible to completely prevent artefacts due to the dynamic nature of the task itself.

Artefact and neural sources are separated by an algorithm based on statistics known as independent component analysis (ICA). There are different types of ICA, but the goal is always the same: decompose the mixed channel data into maximally independent sources/components. ICA is performed twice in this study. First, on the continuous, filtered data. Then, automatic artefact rejection is performed, in which outliers are removed. After cleaning the component data, another ICA is performed. The results of the final ICA are then copied to the continuous data, after which the data can be analysed.

The independent components for eight participants were included in the analysis. Two participants were excluded because they stepped with their left foot. Based on the time-domain data, frequency spectrum, spatial location and the dipole representation, similar components are grouped into clusters. Seven clusters were created to get a representation of cortical areas that matches with previously identified involved areas. Permutation based statistics were applied to find differences between conditions for the obtained clusters in time- and time-frequency domain.

Significant differences in time-domain were found at a cluster located centrally at the scalp, around the motor cortex. A positive drift is seen prior to the perturbation in the stepping condition. Based on the latency, the potential looks like a readiness potential. The readiness potential, however, is usually described as a negative shift, although literature also suggests that it can occur as a positive potential. Additionally, in time-domain, a strong negative peak is visible which has been related to error detection. In both conditions this peak is visible; there are no significant differences between conditions. In time-frequency domain, there is significantly higher involvement of the vestibular and visual system during step inhibition. The increased involvement is represented by event-related desynchronisation in the alpha and frequency band around the temporal-occipital area, which is associated with increased activity of those sensory systems. The expected synchronisations and desynchronisations at the central region of the head take place, in accordance with previous literature. It was hypothesised that the magnitude of modulation is higher in the inhibitory condition, but no significant differences between conditions were found.

The dataset used in this study is rather small. Only 8 subjects were included and for some participants, up to 65% of the data was rejected because of artefacts. Although the correspondences in time-domain (negative peak directly after the perturbation) and expected modulation in the described frequency bands were found, more data might provide a better insight in differences between conditions and might require the hypothesis being reconsidered. Differences in the number of dipole-like components and the quality of the dipole representations exist between participants. As a recommendation, more trials and longer delays between trials, in which EEG is recorded during stance, could improve the decompositions as it will make the percentage of rejected data smaller. However, this first study already demonstrates the potency of recording EEG while receiving perturbations by the Radboud Falls Simulator. Although the dataset was rather small, the general findings correspond to what was found in previous research.

1

INTRODUCTION

1.1. BACKGROUND

Falling is one of the major causes of accidental or unintentional injuries worldwide [1]. The World Health Organisation estimates 424,000 fatal falls occur per year and adults older than 65 years are at highest risk. In the 65+ group, about 28-35% suffers at least one fall per year [2]. Falling incidence among stroke survivors is significantly higher compared to healthy elderly [3]. To better understand the reason behind these high numbers, balance control has been subject of neurological research in recent years [4–13]. In order to better understand the neural mechanisms behind balance control, mobile neuroimaging techniques such as functional near-infrared spectroscopy (fNIRS) [4–6] and electroencephalography (EEG) [7, 9–14] have been used during balance experiments. In these studies, the focus was on the moment at which loss of balance occurs [9], cortical changes associated to performance and perturbation intensity [10, 11], and habituation to external balance perturbations [12, 13].

Using fNIRS, active regions in the prefrontal, premotor, supplementary motor and parietal cortical areas were found in both hemispheres, similar to healthy participants, for hemiplegic stroke patients [6]. Mihara *et al.* [6] performed an experiment in which participants received unexpected forward and backward balance perturbations at velocities up to 0.5 m s^{-1} . Additionally, the superior temporal gyrus, in which the vestibular system is represented, showed higher activity related to an increase of task difficulty in a virtual balancing environment [4].

For EEG, during time-domain analysis, changes in event-related potential (ERP) such as the contingent negative variation (CNV) were revealed when cues were given prior to perturbation onset [12, 15]. The CNV is a slow, negative drift in the EEG, which has been related to expectation. An increase of CNV amplitude was also found, related to unpredictability and variability of perturbation magnitude during backward surface translations of varying amplitude [13]. In time-frequency domain, event related spectral perturbations [16] (ERSP) have been observed around different events during balance perturbation experiments: an increase in balancing difficulty has been related to synchronisations in the theta frequency band (4-7 Hz) over the frontal-central area [8] for unpredictable, visually applied balance perturbations. Likewise, theta frequency modulation related to continuous balancing difficulty has been demonstrated in central-parietal regions during bipedal/unipedal stance on surfaces with varying stability [10]. Moreover, theta synchronisation was also found at the moment balance was lost when balancing on a narrow beam and a compensative step was required to restore balance [9]. Sipp *et al.* [9] also demonstrated that during walking on a balance beam, compared to normal treadmill walking, there is significantly lower power in the beta frequency range (13–30 Hz). Additionally, a burst of gamma synchronisation (30-50 Hz) was observed around the frontal-central area, prior to the moment a compensatory action was required to restore balance during self-initiated postural oscillations [7]. During unexpected trials, while keeping the feet in place as a response, delta (0–4 Hz), theta, alpha (8–15 Hz) and beta (16–30 Hz) modulation have been reported around the central-frontal area of the head [8].

1.2. PROBLEM STATEMENT

The previously mentioned studies have investigated the cortical origin of a variety of natural responses, such as stepping, to perturbations. Stepping, however, is not always a possible strategy to recover from a pertur-

bation. Environmental constraints such as lack of space may limit or restrict the ability to step as a response to large perturbations. Additionally, effects of neurological disorders such as stroke or Parkinson's disease (PD) may also constrain stepping capabilities to postural perturbations. For example, stroke survivors prefer stepping with the non-paretic leg, independent of the direction of perturbation [17]. PD patients fall more often than healthy persons within the same age group [3] and the inability to step (freezing) is one of the main causes [18]. Neural activity patterns related to step inhibition have not yet been subject of research. It is of high importance to better understand the neural origin of step inhibition because the group at higher risk (age > 65 [17]) relies most on the stepping strategy, rather than ankle or hip strategies [19], when compared to young, healthy adults and if a compensatory step is inhibited for too long, falling is inevitable. Additionally, suppression of processes responsible for step inhibition may improve the stepping capabilities. In order to do this, step inhibition processes should first be revealed.

1.3. GOAL

The goal of this study is to explore what cortical regions play a role in voluntary step inhibition during balance perturbations. Neuroimaging studies have already provided valuable insight in how the cortex contributes to balance control. Yet, the complete process of controlling balance is not completely known [20]. In this study, EEG is combined with a motion platform to determine the differences between stepping and step inhibition as response to uni-directional balance perturbations. A better understanding of balance control could be helpful in fall prevention training or setting up more effective rehabilitation therapies for people suffering from neurological disorders such as stroke [21]. Comparison of the results of what is known previous balance research with the acquired results in this study, will also provide insight in the feasibility of recording EEG on participants receiving balance perturbations by the specific motion platform used in this study.¹

1.4. APPROACH

To identify cortical regions involved in balance control, an experiment is set up, in which participants receive backward balance perturbations on a moving platform. In half of the number of trials, participants are instructed to inhibit their step. In the other half, participants are allowed to take a step as response to the perturbation. Conditions are randomised throughout the experiment and the instruction is given visually prior to perturbation onset.

High-density EEG is recorded to measure changes in electric potential on the scalp during the experiment. Participants receive balance perturbations by movement of the platform on which they stand at a variable time after the visual cue has been given. The magnitude of the perturbation is equal among all trials and dependent on the subject specific *stepping threshold*. The stepping threshold is defined as the *maximum perturbation acceleration* (in ms^{-2}) *the participant can withstand without making a step*. The stepping threshold is subject specific and is determined prior to the experiment by iteratively increasing perturbation magnitude up to the point the participant fails to keep the feet in place. Perturbations at this intensity introduces a number of challenges to deal with; motion/muscular (EMG) artefacts may spread to the EEG channels because the stepping threshold intensity requires large effort of the participants in order to restore balance.

1.5. HYPOTHESIS

Previous research has shown increased modulation in the theta and gamma frequency bands at the moment balance was lost in the frontal-central and parietal-occipital region, respectively. These modulations should be visible during both balance strategies, however in the feet in place condition, modulation is expected to be larger compared to the stepping strategy condition, as it requires more effort to recover from the perturbation. Theta synchronisation in the frontal-central region has been associated to balancing difficulty in existing literature and should be more present during the step inhibition condition compared to the stepping response. It is hypothesised that there will be a larger modulation in theta, alpha, beta and gamma frequency bands near the central-frontal region of the scalp, during the feet in place strategy trials compared to the stepping response. Higher modulation means event-related synchronisation (ERS) in the case of theta and gamma frequency, whereas the alpha and beta frequency band will show event-related desynchronisation (ERD) during the feet-in-place condition. ERD has been associated to increased cortical processing and is expected to be more present in the step inhibition condition.

¹A pilot of this experiment was also performed with a CVA patient, see Appendix B

2

METHODS

2.1. PARTICIPANTS

Ten healthy volunteers (4 female) participated in this experiment (mean \pm SD: 23.5 ± 3.4 years). None of the participants had any history of neuromuscular diseases or other impairments that limited their participation in the experiment. The experiment was approved by the ethics committee for human research (CMO Arnhem - Nijmegen). All participants signed informed consent prior to the experiment.

2.2. PLATFORM

In this experiment, a dynamic posturography platform, the Radboud Fall Simulator (RFS), is used to study balancing capabilities [22]. The RFS consists of a platform which can quickly accelerate in any desired direction of the transverse plane at magnitudes up to 4.5 ms^{-2} . The participant's response to a perturbation can be captured using a passive, optical motion capture system. Additionally, EMG can be recorded, and force-plates in the platform record the distribution of the participant's weight. In combination with each other, the RFS can be used to safely explore compensatory responses to balance perturbations for healthy people, as well as people suffering from neurological disorders such as Parkinson's disease and stroke. Participants take place at the mid-line of the platform, such that each foot is placed on a different half of the platform such that ground reaction forces can be recorded. For safety purposes, participants wear a harness which is suspended from an overhead track that moves along with the platform during a perturbation. To reduce expectancy during consecutive perturbations, random delays in between trials can be applied. Once these preparations are taken, the researcher can apply the balance perturbations from the user interface computer.

2.3. EXPERIMENTAL PROTOCOL

In this experiment, participants received 100 *backward* perturbations at their specific stepping threshold. During backward perturbations, the platform moves backwards and, as a consequence, the centre of mass of the person on the platform moves forward. In 50 trials, participants are allowed to respond to the perturbation by taking a step. If they decide to take the step, it should be taken directly after the perturbation, without any moment of inhibition. In the other 50 trials, participants try to keep their feet in place and recover from the perturbation by applying a different strategy than stepping.

To reduce EMG/motion artefacts and variance in balance strategies among trials, participants are instructed to use their hands to hold the safety harness in which they are mounted. Not only does this force participants to rely on ankle/hip strategies, it also reduces the chance of muscular artefacts spreading from the shoulders to the EEG cap. Participants hold the harness during the entire EEG recording, such that the arms are positioned equally during baseline and perturbation phase. Prior to the experiment, the stepping threshold is iteratively determined per participant by gradually increasing perturbation intensity up to the point where participants fail to keep their feet in place. An overhead track and harness system is used during the entire experiment to prevent the participants from actual falling.

Participants start from the centre of the platform for all trials. The feet are placed parallel to each other, 10 cm apart, such that each foot is placed on a different half of the platform. Prior to each perturbation, a visual cue is projected on a screen in front of the participant. The cue is given between 5.75 ± 0.5 s prior to



Figure 2.1: Radboud Falls Simulator

perturbation and consists of a green or red square for the step (NR) or feet-in-place (NS) condition, respectively. The cue is shown on the screen for two seconds, after which a delay (duration: 3.75 ± 0.5 s) takes place, followed by the platform perturbation. Figure 2.2 shows the time-course of a trial, which lasts, dependent on perturbation magnitude, about 15 seconds to complete. The time between the end of platform recovery and the start of the next trial always equals 7.5 seconds. The duration of the pauses prior to the perturbation are dependent on each other, as the cue always lasts for two seconds, the pauses sum up to 5.25 seconds per trial. The total trial length depends on the stepping threshold, which is constant across trials but varies across participants. For higher accelerations, it takes longer for the platform to return to the starting position.

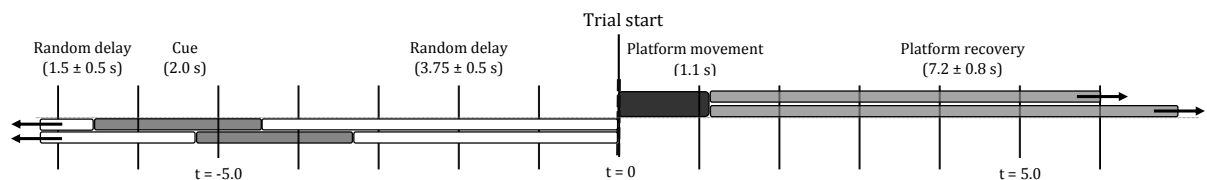


Figure 2.2: Time-course of a trial. The perturbation takes place at $t = 0$. Prior to the perturbation, the cue is provided after which a pause of random duration (3.75 ± 0.5 s) takes place until the perturbation onset. The perturbation itself consists of 0.3 s acceleration, followed by 0.4 s continuous velocity and finally 0.3 s deceleration. The platform then requires time to return to the starting position. This recovery time is dependent on the distance travelled by the platform, which is dependent on the magnitude of acceleration of the perturbation. After the platform is back in starting position, a random pause takes place before the visual cue for the next trial is given.

The trials are divided into five blocks of 20 trials each. Each block contains 10 trials per condition. The order of trials is randomised for each block for all participants. Prior to the first block, a familiarisation session is performed to get participants acquainted with the experiment and instructions, and to minimize possible learning effects to be included in the experiment.

2.3.1. INSTRUCTIONS

Participants are instructed to hold the harness like a backpack during all trials to limit the number of available balance strategies for the participants, to minimize the formation of artefacts and to prevent interference with the cables from the EEG amplifier. By asking them to hold the harness with their hands, participants are limited to using ankle/hip strategies during NS trials. In the NR trials, participants receive the instruction a step is allowed. Additionally, participants are instructed to take the step directly, without any moment of suppression, if they decide to make a step in the NR condition. Moreover, participants are instructed to try

to minimize activity of the facial muscles and to focus their gaze, with normal blinking allowed, on a dot projected on the screen during each block of 20 trials. Participants are informed on the influence of facial expressions on the quality of the EEG data prior to the experiment.

2.4. DATA ACQUISITION

EEG data is recorded using a 128-channel EEG cap (TMSi, Oldenzaal, The Netherlands) at a sampling rate of 2048 Hz and at the common average reference (CAR). The electrode channels are distributed along the scalp according to the international 10:5-system [23]. Electrodes are actively shielded and their recorded signals are amplified with a gain of 20. Artefactual sources were recorded as follows: ocular activity (EOG) (2 channels); one electrode was placed on the between the eyes, slightly above the nasion, to record vertical eye movement, the other at the left temple to record horizontal eye movement. The left mastoid was used as ground for the EEG/EOG channels. Muscular activity of the neck was recorded using four bi-polar derivations placed on the left and right *m. sternocleidomastoideus* and the left and right *m. trapezius*. To improve skin/electrode connection, the skin was cleaned using abrasive gel. The Cz electrode was aligned at 50% of the nasion-inion distance and the left- and right preauricular points. Scalp/electrode connection impedance was reduced by injecting a conductive, water-based gel into the EEG capsules. Electrode impedances were kept below 25 k Ω for the entire experiment.

To allow synchronisation of EEG data and perturbation onset, a digital trigger signal was sent to the EEG amplifier through Matlab. The trigger signal indicates motion of the platform by becoming high as soon as the platform starts moving, and returns to zero after the platform is back in starting position. All EEG, EOG, EMG signals and the trigger signal were recorded in Asalab 4.9.2 software. The trigger signal is also received online in Matlab, where it is used as reference to time visual cues with respect to perturbation offset. An additional signal is sent from Matlab to the EEG amplifier to be able to identify conditions.

A head marker was placed at the right temple to track head motion, which is used during analysis to identify possible correspondence between head motion and EEG, as a measure for motion artefacts [24].

2.5. DATA PREPROCESSING

The recorded EEG data was loaded into EEGLab v13.4.4b [25] (available on: <http://scn.ucsd.edu/eeglab/>) as toolbox in Matlab R2014b. Each block of trials, 20 trials each, is loaded into EEGLab. The data is high-pass filtered at 0.5 Hz and low-pass filtered at 250 Hz using a Hamming windowed sinc FIR filter. Visual inspection is performed to identify and reject channels that show clear motion artefacts or appear as loose electrodes. EMG artefacts are not removed from the data during this initial visual inspection. Particularly around the perturbations events, EMG artefacts are strongly present, so rejection of these segments will remove information from neural activity as well. After bad channels are rejected, the data is rereferenced to the common average reference. All data is then divided into epochs of 0.5 seconds. Next, a first independent component analysis (ICA) is performed using the extended Infomax algorithm [27]. ICA is an algorithm capable of separating mixed signals into maximally independent components. It can be used to separate the recorded EEG channel data, which are mixtures of neural and artefact sources, into those individual sources or components. After Infomax ICA, EEGLab's automatic segment rejection algorithm is applied to remove component epochs containing outliers exceeding the component average ± 6 SD. The division of continuous data into short epochs makes it possible to identify and remove outlier or improbable epochs to obtain cleaner data. An additional, second decomposition is then performed on the remaining epochs, using the Adaptive Mixture Independent Component Analysis (AMICA) [28] algorithm.¹ The preprocessing steps are summarised in Figure 2.3.

2.6. PLATFORM PERFORMANCE

During the experiments, a logfile was created in which successful and unsuccessful trials in NR and NS conditions were noted. Unsuccessful trials will not be taken into account for comparison of differences between conditions. Unsuccessful trials will, however, be included into independent component analysis because although the execution may be unsuccessful, neural structures responsible for balance control will still be activated. Criteria for not including trials in the final analysis are; by visual inspection was checked for short apparent inhibition in the NR condition. If step inhibition was noticed during a NR trial, that specific trial was rejected. Moreover, trials could be excluded if participants kept their feet in place in the NR condition or

¹Matlab preprocessing code has been attached in Appendix C.1

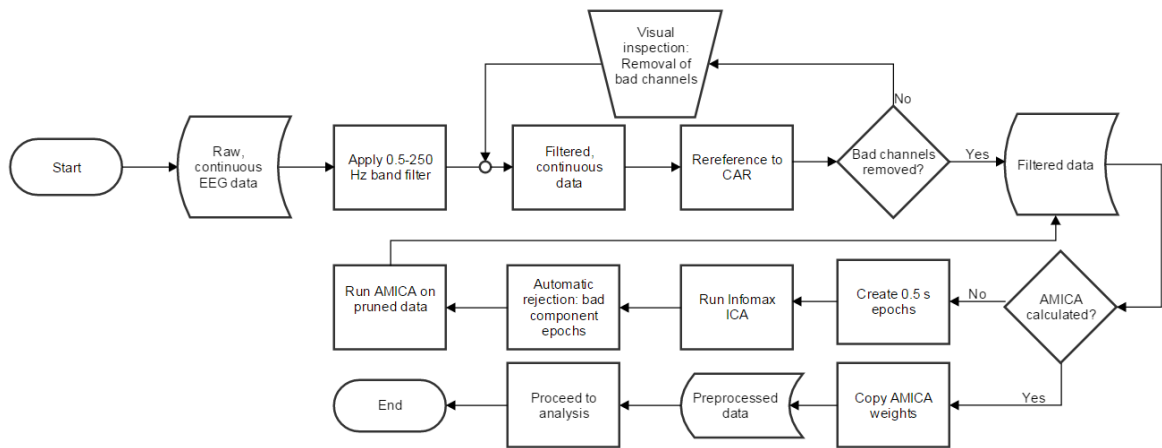


Figure 2.3: Preprocessing steps from raw EEG data to the final step of AMICA.

not keeping the feet in place during NS trials; stepping with the left leg (only right steppers are included in the EEG analysis); using the arms or hands.

2.7. DATA ANALYSIS

2.7.1. SOURCE IDENTIFICATION AND LOCALISATION

To distinguish neural sources from artefacts, the independent components (ICs) resulting from AMICA are judged based on their frequency spectrum and scalp location. Components of interest will appear in scalp maps as concentrated dipolar sources [29] and should have a gradually decreasing power spectrum with peaks at typical EEG frequency bands such as alpha (8-12 Hz) and/or beta (16-30 Hz) range. Section 2.7.1 shows the scalp map and frequency spectrum of an artefact and neural component. Based on the frequency spectra and the topography of the scalp plot, can be concluded that the left image likely has a non-neural origin, indicated by the increasing power spectrum from 20Hz onwards, while the right image clearly shows a peak around 10 – 13Hz and has a topography at the inside the head. These facts taken into account, IC7 is likely not representing an artefact.

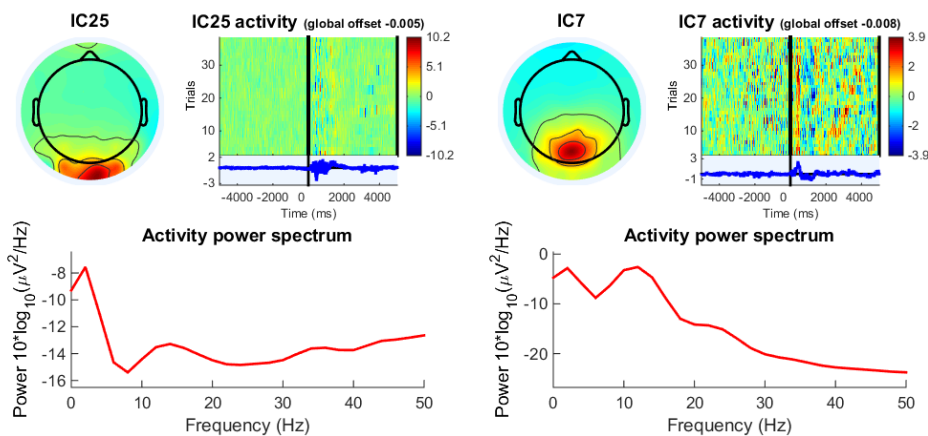


Figure 2.4: Scalp map (left top), component activity per trial (top right) and the power spectrum (bottom) for IC25 (left) and IC7 (right). The location on the scalp map and the increase in power at increasing frequencies indicates that IC25 is likely contaminated with EMG activity. For IC7, the scalp map shows a dipole and the activity power spectrum shows peaks at the alpha and beta band.

A dipole representation of identified neural components is calculated. Dipoles are fitted to a spherical head model (radius: 8.5cm). EEGLab then finds the optimal position in 3D for each IC. The residual variance (RV of a fitted dipole indicates the quality of the fit. A low residual variance means the dipole is well-representing the independent component. Only neural sources with a residual variance below 10% were taken into account during clustering for later analysis in time-domain and time-frequency domain. Brain

structures belonging to the average dipole of each cluster are obtained through Talairach Atlas labels for functional brain mapping [30, 31].

2.7.2. COMPONENT ANALYSIS

The independent components with a residual variance below 10% are verified for outliers. Component trials are rejected if they are indicated as outlier ($\text{mean} \pm 5 \text{ SD}$), compared to the component average. The remaining trials of all components ($\text{RV} < 10\%$) for all subjects are then collected and divided into groups or *clusters*. Clusters are created by grouping similar components in time-domain, time-frequency, dipole location and scalp maps at weighing factors of 1, 1, 10 and 1, respectively, using a k-means algorithm, to allow analysis of component data across subjects. The k-means algorithm randomly creates n means (n is the number of desired clusters). Based on time- and time-frequency domain data, components are associated to the closest mean to create clusters. A new mean of the cluster is then calculated, and the process repeats until convergence is reached.

Analysis is performed in two domains: time- and time-frequency domain. In time-domain, the change of the electric potential over the scalp is studied. In time-frequency domain, the change in power of frequencies over time is studied. The entire analysis is performed in a window of $-1 \text{ s} - 1.5 \text{ s}$ around the perturbation. Statistics between conditions are calculated by permutation statistics, with false detection rate correction. In time-domain, statistic significance is shown if $p < 0.05$. In time-frequency domain, significant differences between conditions are exactly calculated. The difference between conditions are related to a baseline, which is set at the average cluster's components activity of 5 to 3 seconds prior to perturbation onset. Although the cue offset is not fixed in time within this window, this baseline is chosen because the cue offset does not occur at a fixed point in time and any time-locked responses due to the disappearance of the cue should therefore average out. During the baseline window, the participants are always back at their starting position; upright stance while holding the harness like a backpack and focusing their gaze on the target on the screen. Component trials are rejected if they are indicated as outliers ($\text{mean} \pm 5 \text{ SD}$) in EEGLab compared to the trial average.

Event-related Potentials In time-domain, the change of the electric potential of a cluster's components over time is evaluated. This is done by taking the average of all trials, to minimize random noise. The result is a line in time-domain, in which task-related activity will be enhanced. Both conditions are plotted in the same figure and the time at which significant differences occur between conditions are marked by black lines on the (horizontal) time-axis.

Event-related Spectral Perturbations In frequency domain, the change of frequencies over time, also known as event-related spectral perturbations (ERSPs) [32] are analysed. ERSPs show what frequency bands show synchronisation or desynchronisation over time. Each condition is plotted in a separate figure in units of decibels. An change in power of 3 dB means a change in gain of a factor two. Significant differences between conditions are shown in a separate, third figure.

2.7.3. HEAD-MOTION

To address the contribution of head motion artefacts, it was proposed to use head acceleration recordings. By using a Fourier transformation, any time-domain signal can be written as a sum of sinusoids in frequency domain. This means in frequency domain, head accelerations are simply the double time derivatives of head position, such that head motion and acceleration are equal, up to a scaling factor (equal to the squared frequency of each sinusoid). This makes it possible to compare previous results in which head accelerations were correlated with ERSPs to the results of this study. The average of the recorded time-data is calculated and transformed into the frequency domain by a Fourier transform in Matlab. The spectrogram for each participant is then calculated.

3

RESULTS

3.1. DATA PREPROCESSING

Two participants stepped with the left foot as response to perturbations in the NR condition. As a result, the datasets of these two participants are excluded from this analysis. All recorded datasets were visually inspected for outliers, loose electrodes, potential drift and clear motion artefacts. Channels containing these artefacts were rejected before running ICA. On average 13.5 ± 4.8 (mean \pm sd) out of 126 channels were rejected. The continuous data of the remaining channels was then divided into 0.5s epochs before running Infomax ICA. Automatic artefact rejection is applied on the epochs of the component data; if a component epoch exceeds the component's average ± 6 SD, that particular segment is rejected from *all* channels. In some cases, up to 68% of the segmented data was rejected before running AMICA on the pruned, epoched data. This is shown in the 3rd column of Table 3.1, which indicates the percentage of rejected epochs (RE) before running AMICA.

3.2. PLATFORM

Table 3.1 displays the stepping thresholds, the number of successful trials that were included in clustering the total number of successful trials (column 4, 5 and 6). The numbers within parentheses of column 4, 5 and 6 represent the number of trials that were included in AMICA. Dipole representations were calculated for all independent components. If a dipole can be fitted to the component with a residual variance equal to or lower than 10%, it is included for further analysis. The number of components passing below this threshold are listed in column 7. After visual inspection of the components with $RV < 10\%$, trials exceeding the component average ± 5 SD were removed. If more than 10% of the trials of a component was marked as a bad trial, this entire component was removed from further analysis. The number of components that remain and are included for clustering are listed per participant in the last column of Table 3.1.¹

Table 3.1: Data summary of participants stepping with the right foot.

Participant	ST (ms^{-2})	RE (%)	Success: NR	Success: NS	Trial total	ICs
js	1.60	68.0	44 (50)	15 (25)	59 (75)	11
sl	1.05	62.1	49 (50)	27 (28)	76 (78)	16
as	1.50	60.2	49 (50)	39 (39)	88 (89)	17
ls	1.55	60.4	40 (46)	37 (37)	77 (83)	10
lsv	1.25	32.8	18 (49)	35 (45)	53 (94)	13
bl	2.25	61.8	48 (50)	36 (36)	84 (86)	8
jj	1.45	52.5	46 (49)	21 (45)	67 (94)	27
wc	2.05	51.9	37 (49)	19 (40)	56 (89)	7

¹Matlab code for analysis of results across subjects has been attached in Appendix C.2

3.2.1. CLUSTERING

Clustering was performed on 109 components of 8 subjects in total. Measures included for clustering were ERPs (windowed -1000 to 1500 ms around the perturbation, baseline: -5000 to -3000 prior to perturbation), power spectrum (2–40 Hz), scalp topography and dipole location with weight factors of 1, 1, 1 and 10, respectively. Eight clusters were created, of which one consists of outlier components distanced away more than 3 times the standard deviation of the cluster centroids. Seven clusters were created to have a representation of the scalp that matches with cortical areas that were found in previous research. The seven clusters (outlier cluster excluded) are shown in Figure 3.1 from sagittal, transverse and frontal viewpoint.

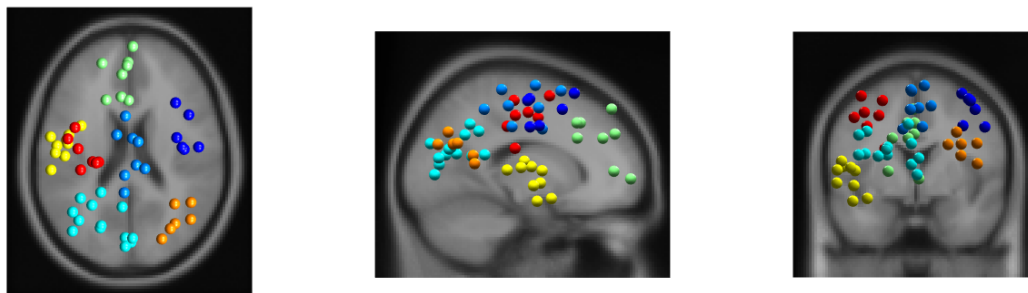


Figure 3.1: Components of 7 clusters, shown in, from left to right: sagittal, transverse and frontal perspective. Each colour represents a different cluster, each sphere a component.

Clusters were found around the middle frontal gyrus (right), temporal lobe (left), medial frontal gyrus (central), precentral gyrus (left), superior temporal gyrus (left), middle temporal gyrus (right). The prefrontal gyrus has been associated to motor control preparation [33]. At the centre of the scalp, the motor cortex is located. Three clusters have been found around the motor area. One at the left and right side (arm control) and one at the midpoint (leg control). Additionally, clusters around the temporal-occipital area have been found for both the left and right hemisphere. Visual and vestibular information is processed in this part of the cerebrum. In Table 3.2, the locations, number of subjects, components and trials are summarised for each considered cluster. The colours in the first column of the table correspond to the colours in Figure 3.1. The number of subjects represented in each cluster is displayed in the third column.

Table 3.2: Summary of clusters: location of mean dipole and number of subjects, components and trials in NR and NS conditions.

Cluster	Location	Subjects	ICs	NR	NS
1	Middle frontal gyrus (r)	6	6	254	173
2	Medial frontal gyrus (c)	6	8	320	200
3	Temporal lobe (l)	8	13	542	390
4	Medial frontal gyrus (c)	6	8	311	233
5	Superior temporal gyrus (l)	6	9	367	256
6	Middle temporal gyrus (r)	4	6	279	184
7	Precentral gyrus (l)	5	7	321	184

3.2.2. TIME-DOMAIN

In time-domain, the spatio-temporal change of electric potential difference is studied. The ERP of the seven considered clusters is shown in Figure 3.2. For all clusters, the baseline period runs from -5 to -3 seconds to the perturbation. The ERP of cluster 5 and 6 still appear to have large amounts of EMG contribution, indicated by the high frequency oscillations. For cluster 6, this is present already before the perturbation. Cluster 1 (right frontal-central) and 7 (left frontal-central) show a gradual decrease in ERP for the NR condition. At the frontal-central brain areas, a negative shift (readiness potential) may indicate preparation of motion. The hand area is represented at the location of the cluster. The measured ERPs could also be a result of hand/arm activation. The locations of the clusters are close to the brain areas that represent the hands. Activity in Cluster 1 and 7 may thus be more related to participants increasing their grasp of the harness as they anticipate to the perturbation.

The post-perturbation increase in ERP for the left and right temporal area (cluster 3, 5 and 6) may reflect an increase in sensory processing of vestibular and visual information. The ERP is larger in the NS condition, compared to NR, which is significant ($p < 0.05$) for the left hemisphere. Although cluster 5 and 6 appear noisier, the ERP has a similar shape as cluster 3. Directly after the perturbation, the ERP is larger in the NS condition. This may reflect additional processing of sensory input from the vestibular and visual system [34]. In cluster 3, representing the left hemisphere, the ERP after the perturbation is significantly higher in NS, compared to NR trials.

Cluster 2, located at the motor cortex (leg area) shows a significant positive drift in the ERP prior to the perturbation in the NR condition. The positive drift looks like a readiness potential, which has been associated to preparation of voluntary motion. The action potential is only visible in the stepping condition. The negative peak at about 150 ms post-perturbation, also named N1 or N100 potential, has been demonstrated before during balance experiments [35–37] and is coupled to error detection. Error detection is done at the same latency and with the same magnitude in both condition. It is the only region in which there are no significant differences between conditions in a window of -250 ms to 400 ms. The error detection in balance perturbations is usually preceded by a positive deflection of the ERP (P1) about $40 - 50$ ms after the perturbation. This ERP is not seen in this data. The positive drift has a much earlier onset (1200 ms before the perturbation) and may be more likely related to the readiness potential [38] for motion initiation. Although the readiness potential is usually seen as a negative shift [12, 38–40], the readiness potential has also been found as a positive drift determined by spontaneous EEG fluctuations [41, 42]. A similar ERP near the Cz location on the scalp was also found in young adults [43].

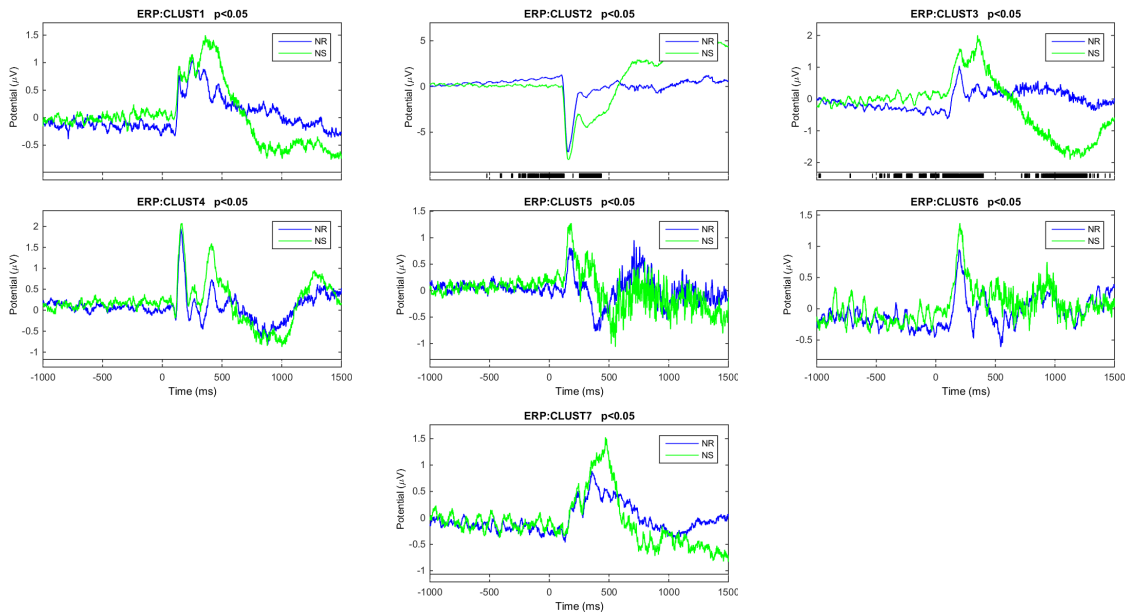


Figure 3.2: Cluster ERPs: Conditions NR and NS are indicated by blue and green, respectively. Significant ($p < 0.05$) differences between conditions are indicated by the black marks above the time-axis. ERPs are centred around the perturbation at $t = 0$.

3.2.3. TIME-FREQUENCY DOMAIN

Event-related spectral perturbations show the change in gain of frequencies over time. The baseline runs from -5 to -3 s to the event and is assumed to be divisive; this means that all changes visible in the figures represent *modulation* of the power of a particular frequency, rather than adding power. The underlying assumption for a divisive baseline is that cortical processes are never turned off, but just active at higher or lower levels. Figure 3.4 shows the average ERSP of each cluster, its dipoles and the dipole average.

All cluster averages show strong event-related synchronisation (ERS) directly after the perturbation in the theta frequency band ($4 - 8$ Hz), although the amount of synchronisation is not equal among all clusters; in all clusters, except cluster 2 (representing the leg area in the motor cortex), higher ERS occurs during NS trials. Cluster 3 and 7 show theta synchronisation is also higher on the left hemisphere controlling the dominant side of the body for right-foot steppers. Cluster 2 does not show any significant differences between conditions. It

shows strong ERS for both conditions up to 25Hz, followed by alpha and high beta ERD after 500ms.

At the parietal-occipital areas high event-related synchronisation is seen in the alpha frequency band (8–15Hz) before the perturbation starts for cluster 3, and 6 in the NR condition. Synchronisation within this band has been related to reduced activity of these sensory systems [44]. At the point the ERS of the alpha frequency band is visible, the participant is already standing in the starting position, focusing on the black screen in front of them. In the view of the participant, effectively, nothing really is happening. The difference in modulation between conditions can then possibly be explained by the additional required sensory information to deal with a perturbation in the NS condition. The sensory system is just not as much deactivated as in the easier stepping condition. Suppression of the alpha frequency band has been connected to enhanced processing of sensory information of the vestibular and visual system. ERS and ERD differences between conditions were found to significant in the alpha frequency band.

Cluster 1 and 7, representing the frontal are of the scalp, show significant differences during preparation towards the perturbation. The alpha frequency band shows synchronisation when NR is compared to NS, for both hemispheres. After the perturbation, the alpha and beta frequency band (16–30Hz) desynchronise. In the NS condition, significant differences in alpha desynchronisation take place. The beta band shows ERD in both conditions. These modulations are likely related to activity of the hand. The hands hold the harness during the experiment. At the moment of the perturbation, the grasp force of the participants is enhanced.

3.3. HEAD MOTION

Head motion is displayed for both conditions in time- and time-frequency domain in Figure 3.3 for one participant. The time-frequency data of all participants is very similar. The additional images have been attached in Appendix A. The time-domain graph shows low-frequency ($f < 2$ Hz) sinusoidal trajectories in both conditions. Head movement in the direction of the platform is larger because of the hip strategy used to overcome the perturbation. This is also resembled by the vertical displacement (z-coordinate, positive upwards) of the head which is greater in the NS condition. In time-frequency domain it is very evident that frequencies up to 5Hz are strongest present in the signal. In the first 0.5s prior to perturbation, the power of these low frequencies is low compared to $t > 0.5$ s post-perturbation. Frequency power above 5Hz is low compared to the lower frequencies; the scale in the time-frequency plots is in decibels, which mean every decrease of 3 dB reduces the power by 50%. Correlation between time-frequency data of head motion and component data has not been calculated because it has been shown that it is not a robust measure of head contamination, since motion artefacts do not spread evenly across the scalp [24]. Event-related spectral perturbations around the delta (0–4 Hz) and low theta (4–8 Hz) frequency band should thus be considered carefully in general, for all components.

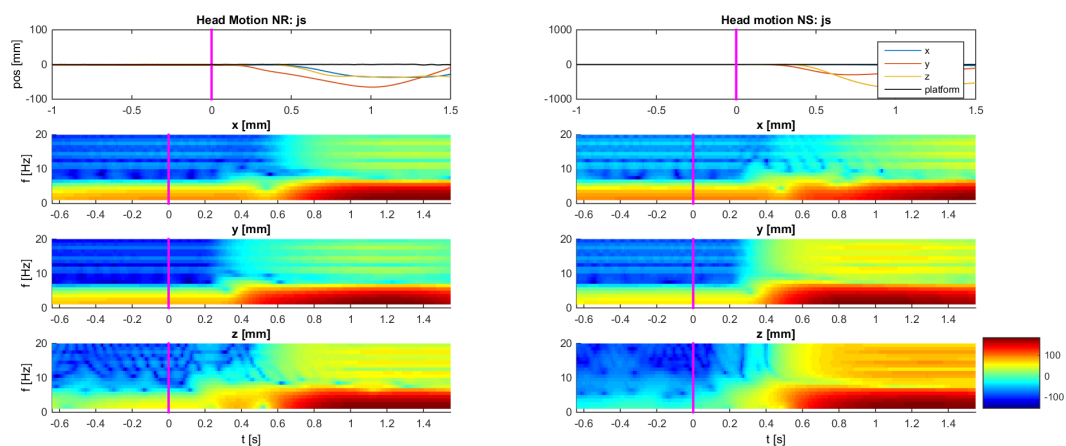


Figure 3.3: Head motion in time-domain (first row) for NR (left) and NS (right) condition. The second, third and fourth row contain the time-frequency data in lateral, forward (direction of perturbation) and vertical direction (x,y,z), for NR (left) and NS (right) condition. The time-domain graph is shown in millimetres. Time-frequency changes are visualised in dB.

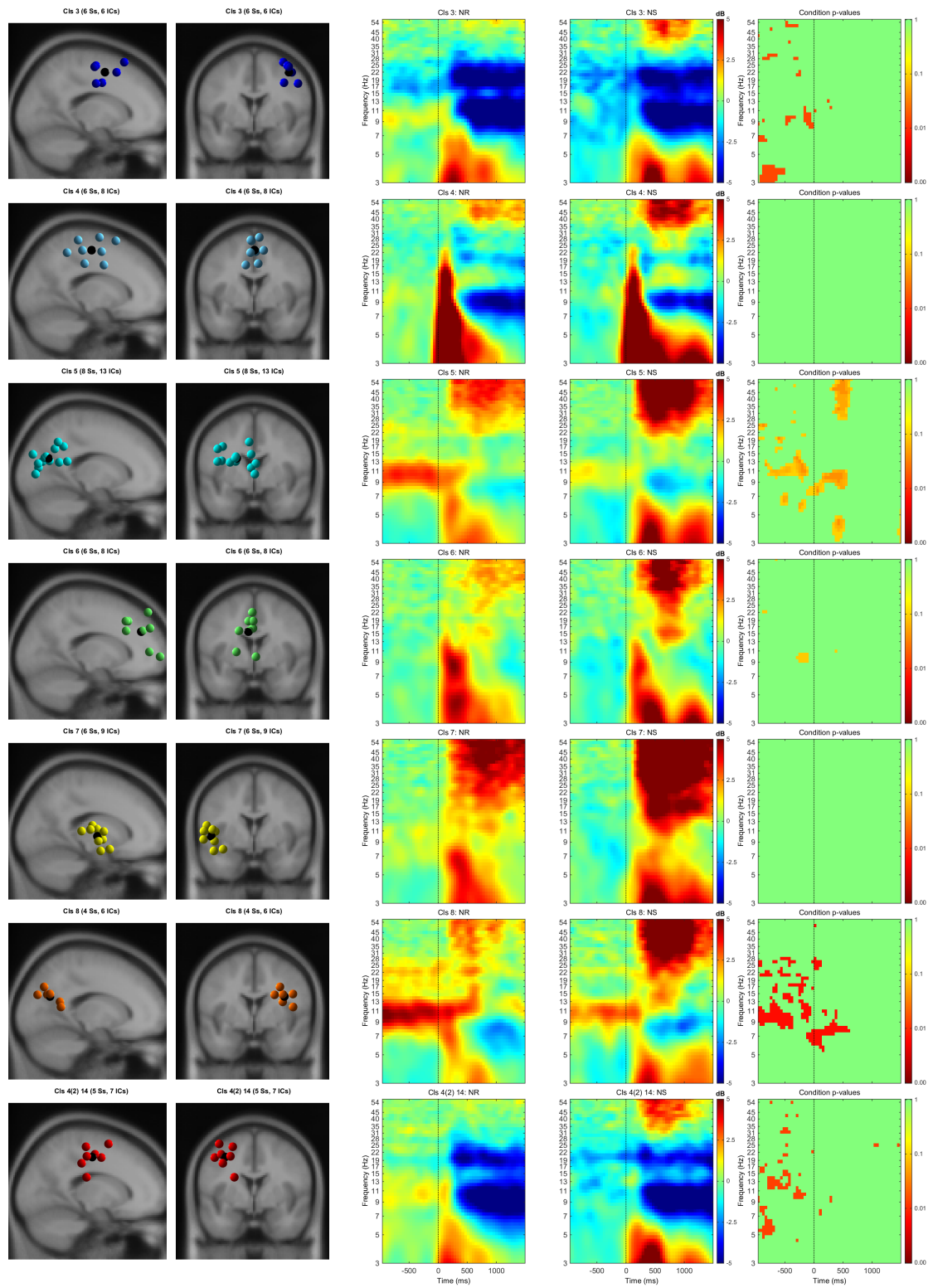


Figure 3.4: Clusters: First and second column: dipole locations of clustered components from sagittal and frontal viewpoint. Each color represents an individual dipole/component. The mean dipole is represented by a black sphere. Third and fourth column: average ERSP for NR and NS condition, respectively. The fifth column shows statistics between conditions; red represents statistical significance.

4

DISCUSSION

4.1. DATA QUALITY

4.1.1. ARTEFACTS

A dynamic task such as keeping balance on a moving platform introduces all kinds of artefacts on the EEG recordings. Muscular activity due to quick recovery responses to the perturbation and, wire movement can severely reduce the quality of the data. A number of preprocessing steps have been taken to optimally minimize these effects. One of the was to show it is possible to record EEG on the RFS. Partially, results correspond to what was found in previous research. This indicates ICA is well-able to separate EMG from EEG activity [29], but motion artefacts are still subject of discussion. Correlation between head accelerations and EEG data cannot reliably indicate if motion artefacts are present [24]. Motion artefacts also do not spread evenly across the scalp, making it even more difficult to be certain about their presence or absence. A solution may be to consider only frequencies that are not contained in accelerometer data, but the head motion frequency spectrum does not linearly translate to EEG artefacts [45]. A combination of head motion and ground reaction forces can introduce motion artefacts during gait. Artefacts due to ground reaction forces may be less applicable here. Only one step is taken per trial in the NR condition, while none are taken in the NS condition. Based on visual inspection, no suspected difference in ERP due to ground reaction forces were found.

Head motion during a balancing experiment is more rapid and covering larger distances compared to treadmill walking, because the balance recovery needs to be performed quickly after the perturbation. Head motion trajectory recordings during the current study show, however, that head motion can be described by frequencies up to about 7Hz. Head accelerations during gait follow a much less smooth trajectory. Direct comparison in frequency domain is an option since, in frequency domain, head acceleration is the double time derivative of position (up to a scaling factor). In addition, for these two conditions and for data analysis directly after the perturbation, participants either keep their feet in place or take a step as response to the perturbation. The ground reaction force of step, if spread as a movement artefact, would show up as a distinguishable peak in the EEG data [45]. Analysis of force plate data would be a way that to find the window in which the step has not taken place yet to make sure ground reaction forces have not influenced the data. It was not included in this study, as visual inspection of the clustering ERPs gave little suspicion for artefacts resulting from ground reaction forces. These artefacts should show up as differences in the ERP after the perturbation, but only in the NR condition. The ERP in the NR condition is at no point significantly larger than the NS ERP, which rules out the existence of motion artefacts originating from ground reaction forces.

4.1.2. ICA

Although ICA was able to find at least 7 components per subject, better decompositions could be obtained if there was more data. The number of required data points depends on the number of channels in the recording. Although there was no trial rejection before AMICA, for some subjects, after removal of unsuccessful and contaminated trials, as little as 56/100 trials in total remained for analysis. Including more artefact-free trials would especially improve the data of ERPs, in which noise reduction is done by averaging. More trials could improve the results of AMICA, but AMICA results could possibly be further improved by adding longer delays in between trials. The underlying assumption is that during stance, the same cortical processes involved in balance control take place, albeit at a lower magnitude. There does not appear to be a clear relation to the

number of components ($RV < 10\%$) and the number of included trials across subjects. For some subjects, up to 60% of 0.5s component epochs were rejected after Infomax ICA. More data allows a better second AMICA decomposition. Longer time in between trials could possibly increase the number or quality of returned components by AMICA. Differences in the capability of a participant to stay focused on the dot on the screen or to keep the facial muscles relaxed may then become less influential. Epochs around the perturbation events are, in general, contaminated by artefacts and epochs around the perturbation were mostly rejected. An increase in ICA quality may therefore be obtained, rather by increasing the delays between trials than increasing the number of trials.

The baseline chosen for the experiment ran from 5 to 3 seconds prior to the perturbation. In this baseline, the cue offset takes place. This baseline was chosen because the cue disappears at randomly distributed points within this period. Any neural activations due to the cue disappearing should average out. Additionally, the 2-second cue is not expected to have any residual effects at this latency, since processing of visual stimuli takes place in approximately the first 500ms after providing the stimulus [46]. Also, the participants have already returned to their starting position within this baseline window. The window before the perturbation taken into consideration is 5 seconds. The only differences in ERSP with the baseline are found at the clusters representing the temporal-occipital area. All other clusters few differences with the baseline period, indicating that the baseline indeed reflects rest EEG.

4.2. TIME-DOMAIN

In this study, two different responses to balance perturbations are recorded, namely stepping and step inhibition. Step inhibition and stepping as response to perturbations have not yet been compared in previous research. ERPs related to loss of balance have been subject to previous research. ERP of the frontal-central region of the scalp have been described by [35–37] as the N1 or N100 ERP, because of the maximum negative deflection 100ms post-perturbation. The N100 ERP appears to be best visible at the Cz electrode. Cluster 2 was found at this exact location. The N1 peak is not preceded by a slow negative potential, which indicates that the latency of the perturbation was unpredictable [36]. In [37], ERPs were recorded during feet-in-place responses to balance perturbations. An ERP at the Cz electrode was recorded, which looks very similar to the ERP acquired by Marlin *et al.* [37] in terms latency. Magnitude of the ERP differs by a factor 2, compared to [37]. Magnitudes of the N1 ERP have been demonstrated to vary with perturbation intensity [47], so this could explain the difference in ERP in this study and [37]. No significant difference between the magnitude of the N1 peak between both conditions was found. The magnitude of the peak has been related to task difficulty. Although the perturbation magnitude between trials is equal, the NS condition requires more effort, as can be concluded from the number of unsuccessful trials. The lack of a significant difference may also follow from adaptation to the perturbations. As the experiment progresses, unsuccessful trials stop from occurring which reduces effects due to differences in task difficulty.

Nonetheless, the N1 potential has been demonstrated to be influenced by the expected postural threat [48]. From the current study it appears as if a small difference in difficulty is experienced by participants, but not significantly. The low magnitude of the N1 potential, may be a consequence of adaptation to the perturbation. Although randomisation of conditions has been applied to reduce these effects, adaptation might still be present. The frequency of unsuccessful trials, particularly in the NS condition, decreases for all participants as the experiment progresses. The ERP of the central cluster also shows that in the NS condition, a positive potential is generated. The positive potential may reflect the readiness potential, which has been found to occur prior to voluntary movement. During step inhibition, the amount of voluntary movement is less, which may explain the absence of the readiness potential, even though muscular activity is required to keep the feet in place. Motion of the participants in this condition is a result of acceleration of the platform, participants themselves are trying their best to keep their feet in place. The readiness potential has often been described as being a negative shift. In the current study, a positive shift is observed, which has been described in recent literature [41, 42]. In these studies, the direction of the readiness potential was described as being subjective to a sum of positive and negative deflections, with often a higher contribution of negative deflections. In this current study, all subjects within the central Cz cluster have shown a positive deflection prior to the perturbation.

In previous balance perturbations, also the CNV has been described. The CNV shows an ERP pattern which starts with a small positive peak after a warning cue, followed by two larger, negative peaks, before a response to a perturbation takes place. The CNV is best visible near neural sources around centre of the head. The observed ERP in this study does not appear to match with previous findings about the CNV. The

ERP shows a positive shift, not a negative one and the latencies are much shorter than what is known of the CNV [12]. The ERP quickly changes from positive to negative as the response takes place. This happens after the perturbation, similar to what Marlin *et al.* [37] find. A possible explanation for the absence of a clear CNV may be the random cue onset, which may average out the first part of the CNV. Also the CNV has been related to expectancy, which may be less applicable since random delays between cues and perturbations introduce uncertainty to reduce predictability.

Significant differences between conditions were found at the left-temporal side of the brain prior to and after the perturbation may, although significant, be a result of a drift in baseline. The NR ERP has a slow negative drift prior to the perturbation. This could also be part of a preparation for the perturbation.

4.3. TIME-FREQUENCY DOMAIN

In accordance with previous literature, increased ERSP are visible at the theta, alpha and low beta (16–30Hz) frequency bands. The gamma band was not taken into consideration at this point, because there appears to be EMG contamination in the clusters. Cluster 3 and 6 contain components located at the *cuneus, precuneus and middle temporal gyrus (and several sub-gyral (temporal lobe))*. These areas have been associated with combined processing of visual and vestibular information [4, 49]. Significant ERSP between conditions were found prior to perturbations at the alpha frequency band, as well as post-perturbation within the first 500 ms after perturbation onset. In general, ERS takes place prior to the perturbation. Synchronisation has been related to reduced activity of sensory systems with respect to baseline [44]. This might reflect gazing at a black screen with nothing else but a dot. In the NS condition, the amount of synchronisation is significantly lower in the alpha and insignificantly in the beta frequency band. Perhaps the differences in the alpha frequency band could be explained as a different degree of awareness. The NR condition is easy to successfully perform. The ERSP plots showed a larger and faster desynchronisation of the alpha frequency band after the perturbation. After the perturbation, the alpha frequency band shows ERD, which has been associated to an increased demand of visual [50] and vestibular [51] processing. The NS condition requires more effort and perhaps the level of activity for the vestibular and visual system is not as far reduced as in the easier NR condition. The baseline used by Ehinger *et al.* [50] was recorded while participants watched a movement presented on a display. In this baseline, the visual system is active, as opposed to when a participant stares at a static, black screen. Besides the baseline difference, the ERSPs of this study and [50] show strong correspondence.

Both alpha and beta suppression take place about 200ms after the event. Strong beta ERD is seen in the sensorimotor area for the hand for both hemispheres and at the central motor area. In previous balance perturbation research, similar suppression of this particular frequency band has been observed. For instance, walking on a balance beam significantly reduced alpha and beta power, compared to normal treadmill walking [9]. Additionally, during assisted treadmill walking when supported and unsupported treadmill walking are compared, desynchronisation in the beta frequency band was larger without support [52]. During the stance phase of the left leg, significant alpha desynchronisation takes place. A similar phenomenon is seen in this study: desynchronisation of the alpha and beta frequency band during stepping with the right leg. There is no difference in magnitude between desynchronisations for the two conditions. Based on the sensorimotor time-frequency activations, it is not possible to discriminate between both conditions in these frequency bands after the perturbation, as no significant differences between conditions were found. Prior to the perturbation, higher alpha desynchronisation can be seen in the left and right hemisphere, around the area where the hand is represented. This could be a result of participants grasping the harness more tightly as preparation to the perturbation and could have been prevented by asking participants to keep their arms crossed. EMG could be used on the arm muscles to verify this explanation.

ERSP in the theta frequency band around the sensorimotor scalp area has previously been associated with balancing difficulty [14]. In this experiment, based on the number of failed trials and the amount of EMG around the perturbation event (judged by visual inspection) can be concluded that the feet in place response is more difficult and requires more effort than the stepping response. An increase in (low) theta synchronisation is indeed visible around the sensorimotor area. The difference is visible in the ERSP plots, but is not significant. From theta modulation, it thus cannot be concluded that participants experienced one condition as more difficult than another. The delta frequency band (1–4Hz) is not discussed here because it is possibly contaminated by motion artefacts. At this point, it is not possible to verify the amount of contamination.

4.4. RECOMMENDATIONS

Based on this study, a recommendation can be made for future research where EEG and the Radboud Falls Simulator are combined. A large part of the data was rejected by the automatic rejection algorithm prior to the AMICA. To reduce the relative loss of data, which was above 65% for some participants, longer delays between perturbations could be a solution. More trials do not necessarily overcome this amount of data rejection because around the perturbation event, EMG artefacts will completely mask the data, especially in the NS condition, and few epochs will survive the automatic artefact rejection. The underlying assumption is that neural processes associated with balance control should after all also be active during normal, upright stance, albeit at a smaller magnitude. Of course, a high number of trials will have a positive impact on the quality of the ERP signals around the event, but more task-related data in itself may improve the decomposition such that the influence of noise is smaller. Additional trials alone will have less effect for the AMICA decomposition, because the automatic rejection algorithm will remove those.

A longer delay will also make it possible to have a more robust baseline, in which no events such as cue offsets, for example, take place. This can only have a positive influence on the ERP and ERSP. Although for some participants, quite a high number of dipole sources were obtained, the differences across subjects are quite large. An increase of the amount of data (more trials or extended delays) might contribute to higher overall quality of the independent component decompositions, less variance between participants and reduced noise in ERPs.

5

CONCLUSION

One of the questions of this experiment was the feasibility of recording EEG while the RFS exerts balance perturbations at stepping threshold intensity. Muscular and motion artefacts were expected and found to be strongly present around the events of interest and it was questionable if the preprocessing steps taken would sufficiently minimize artefacts to recover neural sources from the recordings. In accordance with previous literature, neural sources around the central part of the motor cortex (cluster 2) were found for multiple participants, although not every participant was represented in every cluster.

The obtained time- and time-frequency results show correspondence with previous research; in time-domain, one clear ERP has been found at the central-frontal area which clearly shows the N1 peak. This peak has been found in previous balancing experiments as a result of unpredictable balance perturbations. The N1 peak reflects error detection, which for this type of experiment is the loss of balance. There was no significant in the ERP between conditions after the perturbation. Before the perturbation, the NR condition shows a positive deflection. This positive deflection does not match with previous research; based on the latency of the positive deflection, the ERP appears similar to the readiness potential. Usually, the direction of the RP is negative, although positive readiness potentials have also been observed. The direction of the readiness potential depends on the ratio of positive and negative potentials arising from the cortex. The ratio of negative/positive potentials is larger for the NR condition, but it is not clear why during step inhibition there is an apparent absence of readiness potential.

In time-frequency domain, alpha and beta desynchronisation were found to take place around the central-frontal area of the scalp with respect to baseline. Increased theta synchronisation is also clearly visible directly after the perturbation. There was expected to be a difference between conditions, reflecting task difficulty, but this is not significantly present. Outside the central-frontal region, around the temporal-occipital area, significant differences between conditions take place. During step inhibition, stronger suppression of the alpha frequency band takes place at the temporal-occipital region, which could be a result of an increase of required sensory information to respond adequately to the perturbation. The gamma frequency band was not taken into consideration at this point, because of suspected EMG contamination still being present on the component data. ERSPs in the delta frequency band was also not taken into consideration because it cannot be assured that event-related changes find their origin in neural processes or motion artefacts. The frequency spectrum of head motion itself shows large activation in the delta frequency band. At this moment, there is no robust way of detecting the presence of motion artefacts in this kind of balancing experiment. ERSPs of delta, theta, alpha, beta and gamma frequency bands were hypothesised to take place at a higher magnitude when NS is compared to NR. This cannot be confirmed. Although the experiment confirms modulation of these frequency bands during balance perturbations, only significant differences were found as alpha suppression at the temporal-occipital scalp area.

This study shows the opportunities of using EEG and the Radboud Falls Simulator. The results show correspondence to previous findings in both time- and time-frequency domain. It was hypothesised that the NS condition required larger modulation at theta, alpha beta and gamma frequency bands, but this was not found. For now, the hypothesis is rejected. Also, the origin of the positive deflection at the central cluster in

the NR condition cannot directly be explained. A larger dataset in which the delays between perturbations are increased, as well as the number of trials, are expected to result in better decompositions and more consistency among participants in the retrieved components. These aspects could make it more evident what neural differences exist between compensatory stepping and step inhibition as response to balance perturbations and may require the hypothesis to be reconsidered. Additionally, it will allow a deeper analysis to further unravel the role of the cortex in these processes.

BIBLIOGRAPHY

- [1] World Health Organization, *WHO Global Report on Falls Prevention in Older Age* (World Health Organization, 2008).
- [2] J. A. Stevens, P. S. Corso, E. A. Finkelstein, and T. R. Miller, *The costs of fatal and non-fatal falls among older adults*, *Injury Prevention* **12**, 290 (2006).
- [3] L. Jorgensen, T. Engstad, and B. K. Jacobsen, *Higher incidence of falls in long-term stroke survivors than in population controls: Depressive symptoms predict falls after stroke*, *Stroke* **33**, 542 (2002).
- [4] H. Karim, B. Schmidt, D. Dart, N. Beluk, and T. Huppert, *Functional near-infrared spectroscopy (fnirs) of brain function during active balancing using a video game system*, *Gait & Posture* **35**, 367 (2012).
- [5] M. Mihara, I. Miyai, M. Hatakenaka, K. Kubota, and S. Sakoda, *Role of the prefrontal cortex in human balance control*, *NeuroImage* **43**, 329 (2008).
- [6] M. Mihara, I. Miyai, N. Hattori, M. Hatakenaka, H. Yagura, T. Kawano, and K. Kubota, *Cortical control of postural balance in patients with hemiplegic stroke*, *NeuroReport* **23**, 314 (2012).
- [7] S. Slobounov, M. Hallett, S. Stanhope, and H. Shibasaki, *Role of cerebral cortex in human postural control: an EEG study*, *Clinical Neurophysiology* **116**, 315 (2005).
- [8] J. P. Varghese, A. Marlin, K. B. Beyer, W. R. Staines, G. Mochizuki, and W. E. McIlroy, *Frequency characteristics of cortical activity associated with perturbations to upright stability*, *Neuroscience Letters* **578**, 33 (2014).
- [9] A. R. Sipp, J. T. Gwin, S. Makeig, and D. P. Ferris, *Loss of balance during balance beam walking elicits a multifocal theta band electrocortical response*, *Journal of Neurophysiology* **110**, 2050 (2013).
- [10] T. Hülsdünker, A. Mierau, C. Neeb, H. Kleinöder, and H. Ströder, *Cortical processes associated with continuous balance control as revealed by EEG spectral power*, *Neuroscience Letters* **592**, 1 (2015).
- [11] A. Mierau, T. Hülsdünker, and H. K. Strüder, *Changes in cortical activity associated with adaptive behavior during repeated balance perturbations of unpredictable timing*, *Frontiers in Behavioral Neuroscience* **9**, 1 (2015).
- [12] J. V. Jacobs, K. Fujiwara, H. Tomita, N. Furune, K. Kunita, and F. B. Horak, *Changes in the activity of the cerebral cortex relate to postural response modification when warned of a perturbation*, *Clinical Neurophysiology* **119**, 1431 (2008).
- [13] B. A. Smith, J. V. Jacobs, and F. B. Horak, *Effects of magnitude and magnitude predictability of postural perturbations on preparatory cortical activity in older adults with and without parkinson's disease*, *Experimental Brain Research* **222**, 455 (2012).
- [14] S. M. Slobounov, E. Teel, and K. M. Newell, *Modulation of cortical activity in response to visually induced postural perturbation: Combined vr and EEG study*, *Neuroscience Letters* **547**, 6 (2013).
- [15] W. G. Walter, R. Cooper, V. J. Aldridge, W. C. McCallum, and A. L. Winter, *Contingent negative variation: An electric sign of sensori-motor association and expectancy in the human brain*, *Nature* **203**, 380 (1964).
- [16] S. Makeig, *Auditory event-related dynamics of the EEG spectrum and effects of exposure to tones*, *Electroencephalography and Clinical Neurophysiology* **86**, 283 (1993).
- [17] V. Weerdesteyn, M. d. Niet, H. J. R. van Duijnhoven, and A. C. H. Geurts, *Falls in individuals with stroke*, *JRRD* **45**, 1195 (2008).

- [18] B. H. Wood, *Incidence and prediction of falls in parkinson's disease: a prospective multidisciplinary study*, [Journal of Neurology, Neurosurgery & Psychiatry](#) **72**, 721 (2002).
- [19] L. A. Brown, A. Shumway-Cook, and M. H. Woollacott, *Attentional demands and postural recovery: The effects of aging*, [The Journals of Gerontology Series A: Biological Sciences and Medical Sciences](#) **54**, 165 (1999).
- [20] D. Bolton, *The role of the cerebral cortex in postural responses to externally induced perturbations*, [Neuroscience & Biobehavioral Reviews](#) **57**, 142 (2015).
- [21] J. V. Jacobs, *Why we need to better understand the cortical neurophysiology of impaired postural responses with age, disease, or injury*, [Front. Integr. Neurosci.](#) **8** (2014), 10.3389/fnint.2014.00069.
- [22] J. Nonnekes, D. de Kam, A. C. Geurts, V. Weerdesteyn, and B. R. Bloem, *Unraveling the mechanisms underlying postural instability in parkinson's disease using dynamic posturography*, [Expert Review of Neurotherapeutics](#) **13**, 1303 (2013).
- [23] R. Oostenveld and P. Praamstra, *The five percent electrode system for high-resolution EEG and erp measurements*, [Clinical Neurophysiology](#) **112**, 713 (2001).
- [24] T. Castermans, M. Duvinage, G. Cheron, and T. Dutoit, *About the cortical origin of the low-delta and high-gamma rhythms observed in EEG signals during treadmill walking*, [Neuroscience Letters](#) **561**, 166 (2014).
- [25] A. Delorme and S. Makeig, *EEGlab: an open source toolbox for analysis of single-trial EEG dynamics including independent component analysis*, [Journal of Neuroscience Methods](#) **134**, 9 (2004).
- [26] MATLAB, *version 8.4 (R2014b)* (The MathWorks Inc., Natick, Massachusetts, 2014).
- [27] T.-W. Lee, M. Girolami, and T. J. Sejnowski, *Independent component analysis using an extended infomax algorithm for mixed subgaussian and supergaussian sources*, [Neural Computation](#) **11**, 417 (1999).
- [28] J. A. Palmer, S. Makeig, K. Kreutz-Delgado, and B. D. Rao, *Newton method for the ICA mixture model*, [2008 IEEE International Conference on Acoustics, Speech and Signal Processing](#) (2008), 10.1109/i-cassp.2008.4517982.
- [29] A. Delorme, J. Palmer, J. Onton, R. Oostenveld, and S. Makeig, *Independent EEG sources are dipolar*, [PLoS ONE](#) **7**, e30135 (2012).
- [30] J. Lancaster, L. Rainey, J. Summerlin, C. Freitas, P. Fox, A. Evans, A. Toga, and J. Mazziotta, *Automated labeling of the human brain: A preliminary report on the development and evaluation of a forward-transform method*, [Hum. Brain Mapp.](#) **5**, 238 (1997).
- [31] J. L. Lancaster, M. G. Woldorff, L. M. Parsons, M. Liotti, C. S. Freitas, L. Rainey, P. V. Kochunov, D. Nickerson, S. A. Mikiten, and P. T. Fox, *Automated talairach atlas labels for functional brain mapping*, [Hum. Brain Mapp.](#) **10**, 120 (2000).
- [32] G. Pfurtscheller and F. Lopes da Silva, *Event-related EEG/meg synchronization and desynchronization: basic principles*, [Clinical Neurophysiology](#) **110**, 1842 (1999).
- [33] M.-P. Deiber, E. Sallard, C. Ludwig, C. Ghezzi, J. Barral, and V. Ibañez, *EEG alpha activity reflects motor preparation rather than the mode of action selection*, [Front. Integr. Neurosci.](#) **6** (2012), 10.3389/fnint.2012.00059.
- [34] B. V. Ehinger, P. Fischer, A. L. Gert, L. Kaufhold, F. Weber, G. Pipa, and P. König, *Kinesthetic and vestibular information modulate alpha activity during spatial navigation: a mobile EEG study*, [Front. Hum. Neurosci.](#) **8** (2014), 10.3389/fnhum.2014.00071.
- [35] B. E. Maki and W. E. McIlroy, *Cognitive demands and cortical control of human balance-recovery reactions*, [J Neural Transm](#) **114**, 1279 (2007).

- [36] G. Mochizuki, K. M. Sibley, J. G. Esposito, J. M. Camilleri, and W. McIlroy, *Cortical response associated with the preparation and reaction to full-body perturbations to upright stability*, *Clinical Neurophysiology*, 1626 (2008).
- [37] A. Marlin, G. Mochizuki, W. R. Staines, and W. E. McIlroy, *Localizing evoked cortical activity associated with balance reactions: does the anterior cingulate play a role?* *Journal of Neurophysiology* **111**, 2634 (2014).
- [38] H. Shibasaki and M. Hallett, *What is the Bereitschaftspotential?* *Clinical Neurophysiology* **117**, 2341 (2006).
- [39] S. Vaez Mousavi and R. J. Barry, *Positive and negative shifts of the readiness potential: preparatory effects*, *International Journal of Psychophysiology* **15**, 105 (1993).
- [40] J. C. Eccles, *The initiation of voluntary movements by the supplementary motor area*, *Arch Psychiatr Nervenkr* **231**, 423 (1982).
- [41] H.-G. Jo, T. Hinterberger, M. Wittmann, T. L. Borghardt, and S. Schmidt, *Spontaneous EEG fluctuations determine the readiness potential: is preconscious brain activation a preparation process to move?* *Experimental Brain Research* **231**, 495 (2013).
- [42] H.-G. Jo, M. Wittmann, T. Hinterberger, and S. Schmidt, *The readiness potential reflects intentional binding*, *Front. Hum. Neurosci.* **8** (2014), 10.3389/fnhum.2014.00421.
- [43] R. Duckrow, *Stance perturbation-evoked potentials in old people with poor gait and balance*, *Clinical Neurophysiology* **110**, 2026 (1999).
- [44] G. Pfurtscheller, A. Stanák, and C. Neuper, *Event-related synchronization (ers) in the alpha band - an electrophysiological correlate of cortical idling: A review*, *International Journal of Psychophysiology* **24**, 39 (1996).
- [45] J. E. Kline, H. J. Huang, K. L. Snyder, and D. P. Ferris, *Isolating gait-related movement artifacts in electroencephalography during human walking*, *Journal of Neural Engineering* **12**, 046022 (2015).
- [46] S. H. Patel, *Characterization of n200 and p300: Selected studies of the event-related potential*, *Int. J. Med. Sci.*, 147 (2005).
- [47] G. Mochizuki, S. Boe, A. Marlin, and W. McIlroy, *Perturbation-evoked cortical activity reflects both the context and consequence of postural instability*, *Neuroscience* **170**, 599 (2010).
- [48] A. L. Adkin, A. D. Campbell, R. Chua, and M. G. Carpenter, *The influence of postural threat on the cortical response to unpredictable and predictable postural perturbations*, *Neuroscience Letters* **435**, 120 (2008).
- [49] J. Ventre-Dominey, *Vestibular function in the temporal and parietal cortex: distinct velocity and inertial processing pathways*, *Front. Integr. Neurosci.* **8** (2014), 10.3389/fmint.2014.00053.
- [50] B. V. Ehinger, P. Fischer, A. L. Gert, L. Kaufhold, F. Weber, G. Pipa, and König, *Kinesthetic and vestibular information modulate alpha activity during spatial navigation: a mobile EEG study*, *Frontiers in Human Neuroscience* **8**, 1 (2014).
- [51] S. Gale, M. Prsa, A. Schurger, A. Gay, A. Paillard, B. Herbelin, J.-P. Guyot, C. Lopez, and O. Blanke, *Oscillatory neural responses evoked by natural vestibular stimuli in humans*. *J Neurophysiol*, jn.00153.2015 (2015).
- [52] J. Wagner, T. Solis-Escalante, P. Grieshofer, C. Neuper, G. Müller-Putz, and R. Scherer, *Level of participation in robotic-assisted treadmill walking modulates midline sensorimotor EEG rhythms in able-bodied subjects*, *NeuroImage* **63**, 1203 (2012).

A

HEAD MOTION PLOTS

The figures in this appendix contain the head motion data in NR and NS conditions for the participants *as*, *bl*, *jj*, *ls*, *lsu*, *sl*, *wc*. Head motion data is presented in time-domain and in time-frequency domain. All time-frequency domain figures are displayed in decibels.

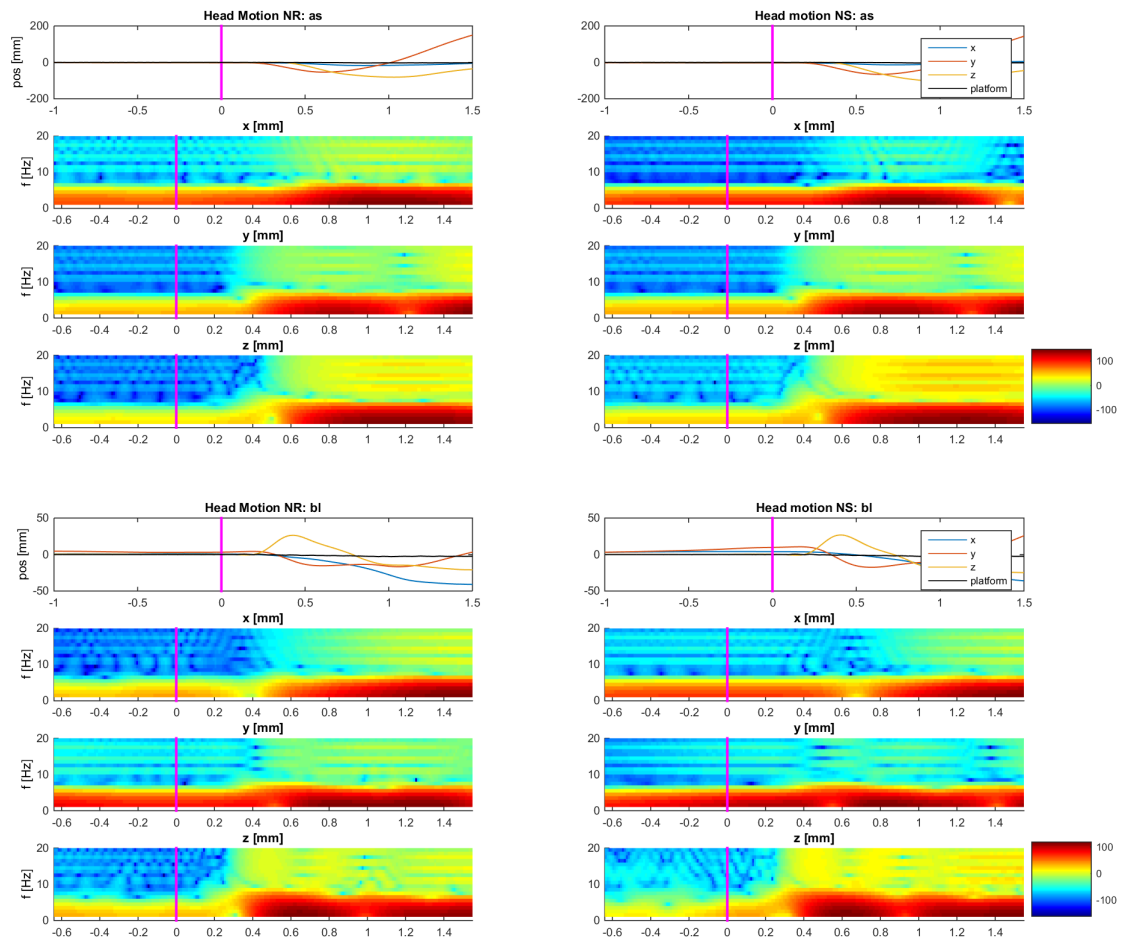


Figure A.1: Head motion data of participant *as* (top) and *bl* (bottom).

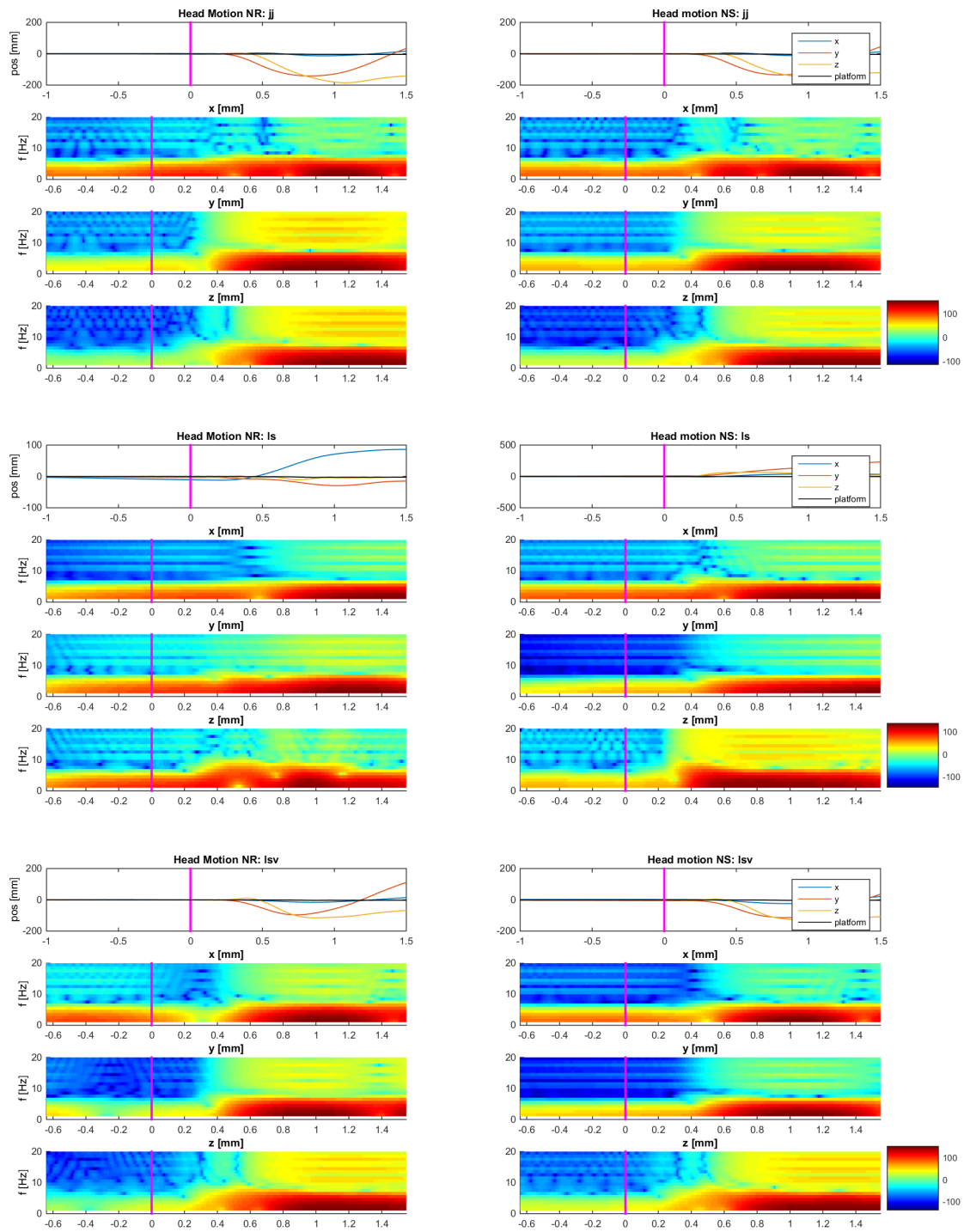


Figure A.2: Head motion data of participant *jj* (top), *ls* (middle) and *lsv* (bottom).

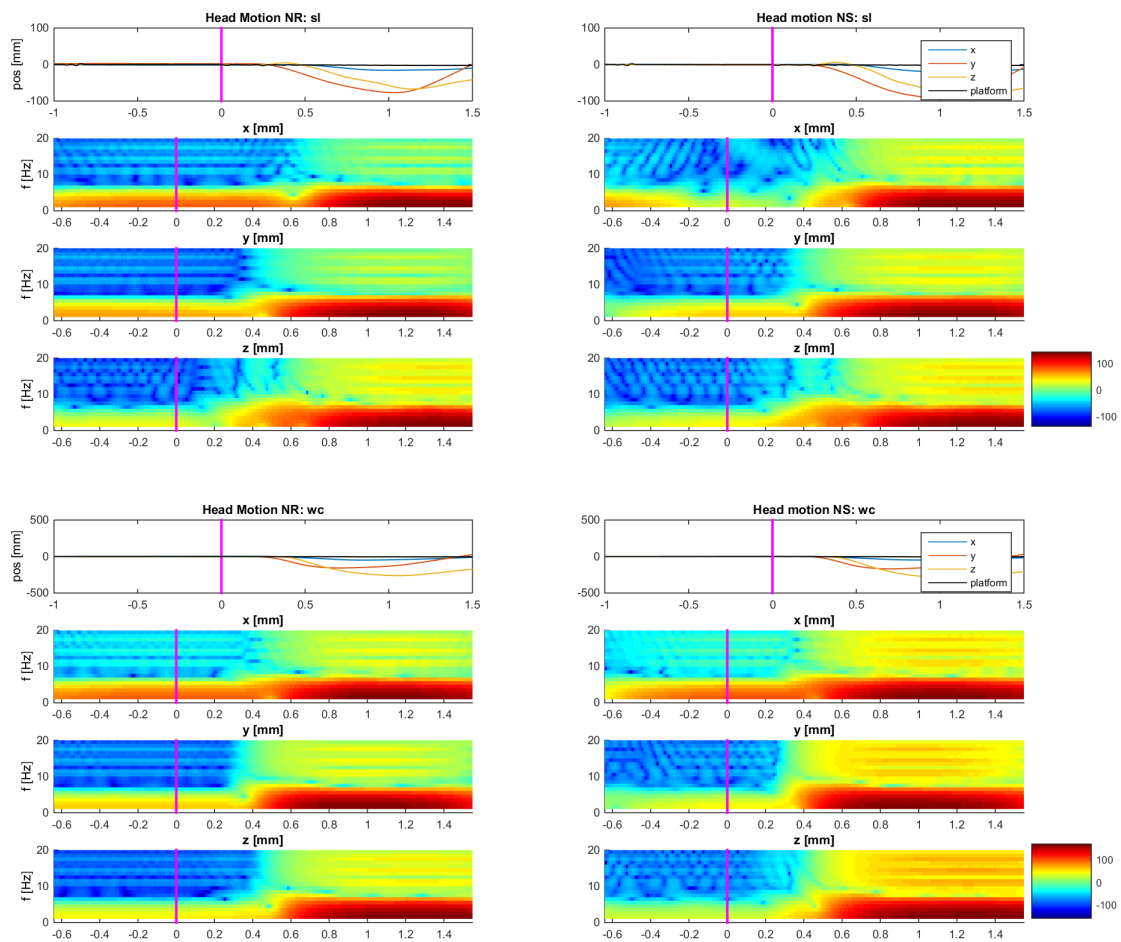


Figure A3: Time- and time-frequency domain plots of *sl* (top) and *wc* (bottom).

B

CVA PILOT

As a pilot study, the experiment performed by 10 healthy, young adults is also performed by one cerebrovascular accident (CVA) patient. The stroke experienced by the participant has affected the left hemisphere. Motor control of the right side of the body is affected. The participant steps with the left leg. The feasibility study should provide insight if adjustments are required when people suffering from neuromuscular disorders participate. Besides this technical objective, the preprocessing methods are also tested to see if a similar result can be obtained as for healthy young participants. For methods, please refer to Chapter 2.

B.1. RESULTS

Six clean neural components with a RV < 10% have been obtained in this pilot experiment. The components are shown in Figure B.1. From these images it becomes clear that mostly the left (affected) hemisphere is represented. The neural structures, from Talairach coordinates [30, 31] represented are: cingulate gyrus (r), middle occipital gyrus (l), frontal lobe (l), insula (l) and the temporal lobe (l). For this analysis, the six components with the lowest residual variance were picked.

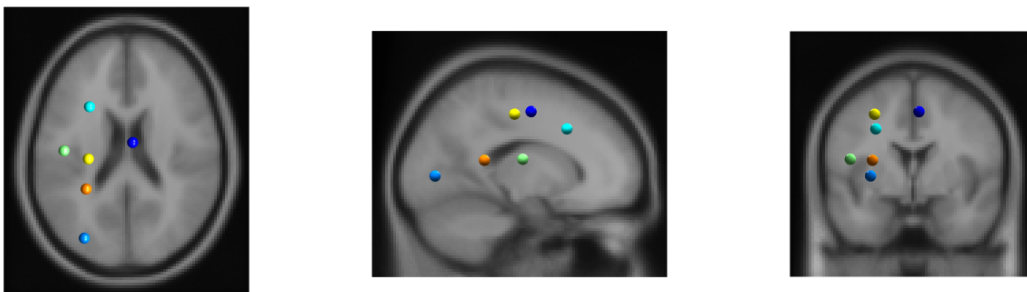


Figure B.1: Six components', shown in, from left to right: sagittal, transverse and frontal perspective. Each colour represents a different component.

The ERPs are visualised in Figure B.2. Component 2, the cingulate gyrus, shows what will likely be the N1 potential as response to unexpected perturbations.

In time-frequency domain, alpha (8 – 15Hz) desynchronisation can be seen at the occipital area of the scalp. This kind of desynchronisation has been related to an increase in processing visual and vestibular information and reflects the higher difficulty of the NS condition, compared to NR. Component 6, representing the left central-frontal region of the scalp, shows alpha and low beta (16 – 30Hz) desynchronisation which is especially evident in the NS condition. In the NR condition, the desynchronisation does not take place over the entire alpha frequency band. In contrast with the NS condition, synchronisation takes place at the low beta frequency band.

These results indicate the feasibility of recovering dipole components from EEG recordings of a CVA patient on the Radboud Falls Simulator (RFS). More pilots are required in order to accurately tell how this pilot compares to the 8 healthy young subjects. Six components were obtained, but only at the affected hemi-

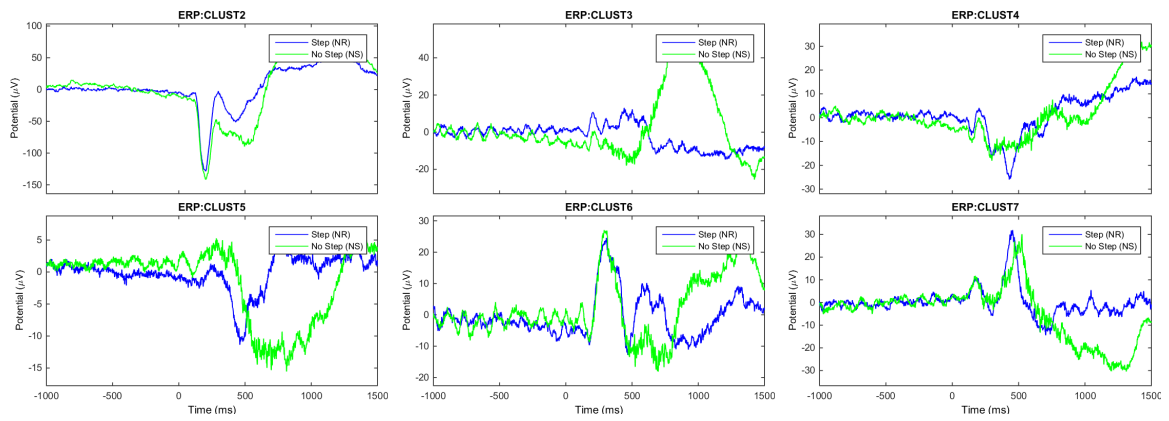


Figure B.2: Cluster ERPs: Conditions NR and NS are indicated by blue and green, respectively. ERPs are centred around the perturbation at $t = 0$.

sphere, which does not control stepping with the left foot. The high magnitude of the ERP signals may indicate the presence of artefacts.

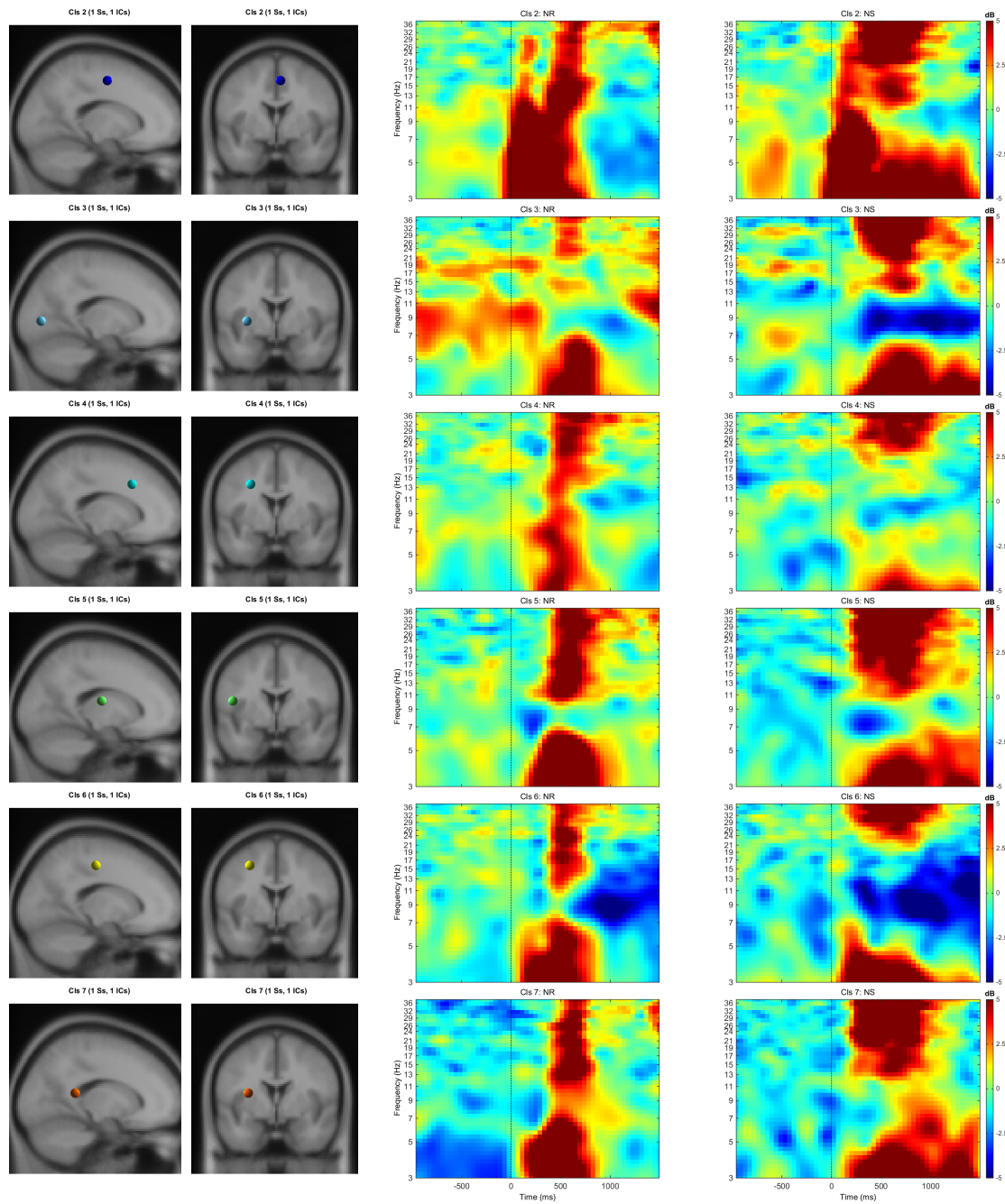


Figure B.3: Component results. First column: dipole locations of components from sagittal viewpoint. Second column: dipole location of components from frontal perspective. Third and fourth column: average ERSP for NR and NS condition, respectively.

C

MATLAB CODE

C.1. PREPROCESSING

```
%%

% -- parameters
% Every subject has their own code and fileList. Sometimes,
% <subject_code>_testNijmegen_002 is not used because of too many
% unsuccessful trials during NS condition.

% Create cell arrays of subject codes and filenames
% Every participant has its own fileList, subject_code and an array with
% channels to be rejected (after visual inspection is performed)

%%% JS %%%
fileList = {'js_testNijmegen_001' 'js_testNijmegen_002' 'js_testNijmegen_003'
            'js_testNijmegen_004' 'js_testNijmegen_005' 'js_testNijmegen_006'};
subject_code = 'js';
channels2reject = [28, 56, 83, 85, 87, 14, 93, 94, 95, 107, 123, 126:132];
channels2reject = sort(channels2reject);
channelRejection(1,:) = {channels2reject};
subjects{1} = subject_code;
files{1,:} = fileList;
mergedFiles{1,:} = {[subject_code '_continuous_merged.set']};

%%

%%% SL %%%
fileList = {'sl_testNijmegen_001' 'sl_testNijmegen_002' 'sl_testNijmegen_003'
            'sl_testNijmegen_004' 'sl_testNijmegen_005' 'sl_testNijmegen_006'};
subject_code = 'sl';
channels2reject = [13 14 17 19 94 110 33 18 71 29 66 129:132];
channels2reject = sort(channels2reject);
channelRejection(2,:) = {channels2reject};
subjects{2} = subject_code;
files{2,:} = fileList;
mergedFiles{2,:} = {[subject_code '_continuous_merged.set']};

%%

%%% AS %%%
fileList = {'as_testNijmegen_001' 'as_testNijmegen_003' 'as_testNijmegen_004'
            'as_testNijmegen_005' 'as_testNijmegen_006' 'as_testNijmegen_007'};
subject_code = 'as';
channels2reject = [14 18 68 111 129:132];
```

```

channels2reject = sort(channels2reject);
channelRejection(3,:) = {channels2reject};
subjects{3} = subject_code;
files{3,:} = fileList;
mergedFiles{3,:} = {[subject_code '_continuous_merged.set']};

%%% EL %%%
fileList = {'el_testNijmegen_001' 'el_testNijmegen_002' 'el_testNijmegen_003'
            'el_testNijmegen_004' 'el_testNijmegen_005' 'el_testNijmegen_006'};
subject_code = 'el';
channels2reject = [8 14 18 29 30 33 37 107 82 121 122 94 127 96 72 68 57 129:132];
channels2reject = sort(channels2reject);
channelRejection(4,:) = {channels2reject};
subjects{4} = subject_code;
files{4,:} = fileList;
mergedFiles{4,:} = {[subject_code '_continuous_merged.set']};

%%% CH %%%
fileList = {'ch_testNijmegen_001' 'ch_testNijmegen_002' 'ch_testNijmegen_003'
            'ch_testNijmegen_004' 'ch_testNijmegen_005' 'ch_testNijmegen_006'};
subject_code = 'ch';
channels2reject = [109 18 35 3 33 52 71 67 6 129:132];
channels2reject = sort(channels2reject);
channelRejection(5,:) = {channels2reject};
subjects{5} = subject_code;
files{5,:} = fileList;
mergedFiles{5,:} = {[subject_code '_continuous_merged.set']};

%%% LS %%%
fileList = {'ls_testNijmegen_001' 'ls_testNijmegen_003' 'ls_testNijmegen_004'
            'ls_testNijmegen_005' 'ls_testNijmegen_006' 'ls_testNijmegen_007'};
subject_code = 'ls';
channels2reject = [56 77 64 81 80 108 129:132];
channels2reject = sort(channels2reject);
channelRejection(6,:) = {channels2reject};
subjects{6} = subject_code;
files{6,:} = fileList;
mergedFiles{6,:} = {[subject_code '_continuous_merged.set']};

%%% LSV %%%
fileList = {'lsv_testNijmegen_001' 'lsv_testNijmegen_003' 'lsv_testNijmegen_004'
            'lsv_testNijmegen_005' 'lsv_testNijmegen_006' 'lsv_testNijmegen_007'};
subject_code = 'lsv';
channels2reject = [18 124 125 126 29 32 91 92 93 28 31 1 97 129:132];
channels2reject = sort(channels2reject);
channelRejection(7,:) = {channels2reject};
subjects{7} = subject_code;
files{7,:} = fileList;
mergedFiles{7,:} = {[subject_code '_continuous_merged.set']};

%%% FB %%%
fileList = {'fb_testNijmegen_001' 'fb_testNijmegen_002' 'fb_testNijmegen_003'
            'fb_testNijmegen_004' 'fb_testNijmegen_005' 'fb_testNijmegen_006'};
subject_code = 'fb';
channels2reject = [14 33 79];
channels2reject = sort(channels2reject);
channelRejection(8,:) = {channels2reject};

```



```

%%%%%%%%%%%%%%%%%%%%%%%%%%%%%%%%%%%%%%%%%%%%%%%%%%%%%%%%%%%%%%%%%%%%%%%%
%%% 1) Low/High-pass filter all the data
%%% 2) Rereference to common average reference
%%% 3) Load channel labels
%%% 4) Load events per dataset
%%% 5) Visually inspect raw signals and remove bad portions
%%% 6) Identify bad channels
%%% 7) Create 0.5 s epochs
%%% 8) Run FastICA
%%% 9) Perform visual inspection on the components
%%% 10) Visually inspect and reject epochs
%%% 11) Perform a second ICA (AMICA)
%%% 12) Inspect components from the 2nd decomposition

%%%%%%%%%%%%%%%%%%%%%%%%%%%%%%%%%%%%%%%%%%%%%%%%%%%%%%%%%%%%%%%%%%%%%%%%
%%%%%%%%%%%%%%%%%%%%%%%%%%%%%%%%%%%%%%%%%%%%%%%%%%%%%%%%%%%%%%%%%%%%%%%%
%%%%%%%%%%%%%%%%%%%%%%%%%%%%%%%%%%%%%%%%%%%%%%%%%%%%%%%%%%%%%%%%%%%%%%%%
%%%%%%%%%%%%%%%%%%%%%%%%%%%%%%%%%%%%%%%%%%%%%%%%%%%%%%%%%%%%%%%%%%%%%%%%

for subid = length(files)
fileList = files{subid};
subject_code = subjects{subid};
%%
for numF = 1:length(fileList)

file_name = fileList{numF}; % 1 = resting state
clear head eeg trg trig_type trig

% -- read header and data
head = read_eep_cnt([ file_name '.cnt'],1,1);
eeg = read_eep_cnt([file_name '.cnt'],1,head.nsample);

fs = eeg.rate;
eeg = eeg.data;

%%
evt = [];

% -- read triggers and create classes (GO/NOGO)
trg = read_eep_trg([file_name '.trg']);

trig_type = [trg.type];
trig = [trg.offset];
disp(num2str(numF));
if sum( trig_type == platformOnset ) > 0

clear new_trig new_type trigList
new_trig = find(trig_type == platformOnset);
indeces = new_trig;% platform movement Onset
new_cue = find(trig_type ~= classTrigger); % non-cue triggers
temp_cue = new_cue(1:length(new_cue))+1; % vector with first entries of cue, remove the last
        entry (out of range, no cue there)

% There is only interest in the pause onset, cue onset, cue offset
% and the start of the platform. There should thus be 4 triggers
% per trial. Except for the first trial; there is only cue on- and

```

```

% offset and the start of the trial
iii = 1;
% Retrieve EVENT triggers: PLATFORM ONSET and CONDITION IDENTIFIERS
for ii = 1

if temp_cue(ii+1) - temp_cue(ii) == 3
new_cue(ii) = temp_cue(ii); % Cue onset
new_cue(ii+1) = temp_cue(ii)+1; % Cue end
trigList(1).type = 2; %% START CUE NS
trigList(2).type = 4; %% END CUE NS
trigList(1).latency = trig(temp_cue(ii));
trigList(2).latency = trig(temp_cue(ii)+1);
trigList(1).condition = {'StartCueNS'};
trigList(2).condition = {'EndCueNS'};
%           disp('3')
elseif temp_cue(ii+1) - temp_cue(ii) == 5
new_cue(ii) = temp_cue(ii);
new_cue(ii+1) = temp_cue(ii) + 3;
trigList(1).type = 3; %% START CUE NR
trigList(2).type = 5; %% END CUE NR
trigList(1).latency = trig(temp_cue(ii));
trigList(2).latency = trig(temp_cue(ii)+2);
trigList(1).condition = {'StartCueNR'};
trigList(2).condition = {'EndCueNS'};
%           disp('5')
end
end
i = 3;
for ii = 2:1:length(temp_cue)-1
if temp_cue(ii+1) - temp_cue(ii) == 4
disp('NS condition')
new_cue(i) = temp_cue(ii); % start delay
trigList(i).type = 1; %% PLATFORM BACK
trigList(i+1).type = 2; %% START CUE NS
trigList(i+2).type = 4; %% END CUE NS
trigList(i).latency = trig(temp_cue(ii));
trigList(i+1).latency = trig(temp_cue(ii)+1);
trigList(i+2).latency = trig(temp_cue(ii)+2);
new_cue(i+1) = temp_cue(ii)+1; % start cue
new_cue(i+2) = temp_cue(ii)+2; % end cue
trigList(i).condition = {'delay'};
trigList(i+1).condition = {'StartCueNS'};
trigList(i+2).condition = {'EndCueNS'};

elseif temp_cue(ii+1) - temp_cue(ii) == 6
disp('Step condition')
new_cue(i) = temp_cue(ii); % start delay
new_cue(i+1) = temp_cue(ii)+1; % Start cue
new_cue(i+2) = temp_cue(ii)+3; % End cue
trigList(i).type = 1; %% PLATFORM BACK
trigList(i+1).type = 3; %% START CUE NR
trigList(i+2).type = 5; %% END CUE NR
trigList(i).latency = trig(temp_cue(ii));
trigList(i+1).latency = trig(temp_cue(ii)+1);
trigList(i+2).latency = trig(temp_cue(ii)+3);
trigList(i).condition = {'delay'};
trigList(i+1).condition = {'StartCueNR'};
trigList(i+2).condition = {'EndCueNR'};

end
i = i+3;

```

```

end
ig(1:(length(new_trig))) = 1;

new_trig = trig(new_trig);
lim = length(trigList);
for i = lim+1:lim+length(new_trig);
trigList(i).latency = new_trig(i-lim);
ii = i - lim;
if temp_cue(ii+1) - temp_cue(ii) == 3 || temp_cue(ii+1) - temp_cue(ii) == 4
trigList(i).condition = 'NS';
trigList(i).type = 10; %% 10 = NS
else
trigList(i).condition = 'NR';
trigList(i).type = 20; %% 20 = NR
end
end
trigFields = fieldnames(trigList);
trigCell = struct2cell(trigList);
sz = size(trigCell);

trigCell = reshape(trigCell, sz(1), []);
trigCell = trigCell.';
trigCell = sortrows(trigCell,2);
trigCell = reshape(trigCell.', sz);
trigSorted = cell2struct(trigCell, trigFields,1);

evt = trigSorted;
evt = struct2cell(evt);
sz = size(evt);
evt = reshape(evt, sz(1), []);
evt = evt.';
evt_labels = evt(:,3);
evt = evt(:,1:2); % Array containing all event information
%     evt = fliplr(evt);
end
clear numTrial trig_type trig temp_cue
%% Import datasets
eeglab('redraw');
EEG = pop_importdata('dataformat','array','nbchan',0,'data','eeg', ...
'setname', file_name , 'srate', fs , 'subject', subject_code , 'pnts',0,'xmin',0);
% Create a new set
[ALLEEG EEG CURRENTSET] = pop_newset(ALLEEG, EEG, 0,'gui','off');
EEG = eeg_checkset( EEG );
% If event information is available
if ~isempty(evt)
% Import events to dataset
EEG = pop_importevent( EEG, 'event', evt , 'fields',{ 'type', 'latency', 'conditions'
}, 'timeunit', NaN);
[ALLEEG EEG] = eeg_store(ALLEEG, EEG, CURRENTSET);
end

% re-reference to common average
EEG = pop_reref( EEG, []);
[ALLEEG EEG CURRENTSET] = pop_newset(ALLEEG, EEG, 1,'overwrite','on','gui','off');
[ALLEEG EEG CURRENTSET] = eeg_store(ALLEEG, EEG, CURRENTSET);
EEG = eeg_checkset( EEG );
disp(' CAR recomputed!')

% lowpass filter
EEG = eeg_checkset( EEG );
EEG = pop_eegfiltnew( EEG, highpass_cutoff, lowpass_cutoff);

```

```

[ALLEEG EEG CURRENTSET] = pop_newset(ALLEEG, EEG, 1, 'overwrite', 'on', 'gui', 'off');

%% save filtered, rereferenced dataset

EEG = pop_saveset( EEG, 'filename', [ file_name '_rej_preICA.set'], ...
'filepath', pwd);
[ALLEEG EEG] = eeg_store(ALLEEG, EEG, CURRENTSET);
STUDY = []; CURRENTSTUDY = 0; ALLEEG = []; EEG=[]; CURRENTSET=[];
eeglab('redraw');

% Store filenames, will be used to merge all individual datasets into one big file
fileList{numF} = [ file_name '_rej_preICA.set'];

% Perform visual inspection, remove bad segments, select channels
end

%% merge datasets
eeglab('redraw');
EEG = pop_loadset('filename',fileList,'filepath',pwd);
[ALLEEG EEG CURRENTSET] = pop_newset(ALLEEG, EEG, 0, 'study', 0);
EEG = eeg_checkset( EEG );
EEG = pop_mergeset( ALLEEG, [1:length(fileList)], 0);
% Create a new set
[ALLEEG EEG CURRENTSET] = pop_newset(ALLEEG, EEG, length(fileList), 'savenew', [subject_code
'_testNijmegen_rej_preICA.set'], 'gui', 'off');
ALLEEG = pop_delset( ALLEEG, [1:numF] );
% Save it under a new name
EEG = pop_saveset( EEG, 'filename', [ subject_code '_testNijmegen_continuous_merged.set'], ...
'filepath', pwd);
[ALLEEG EEG] = eeg_store(ALLEEG, EEG, CURRENTSET);

STUDY = []; CURRENTSTUDY = 0; ALLEEG = []; EEG=[]; CURRENTSET=[];

end

%% Continuous merged set inspection
% Identify bad channels and add them in the header file

for ii = 1:length(subjects)
% Load the dataset
subject_code = subjects{ii};
disp(['Current set: ' subject_code]);
EEG = pop_loadset('filename', [subject_code
'_testNijmegen_continuous_merged.set'], 'filepath', pwd);
EEG = pop_saveset(EEG, 'savemode', 'resave');
[ALLEEG EEG] = eeg_store(ALLEEG, EEG, CURRENTSET);
EEG = eeg_checkset(EEG);
% Visual inspection of channel data
disp('Visual inspection, write channels to be rejected in vector');
pop_eegplot(EEG)
pause
STUDY = []; CURRENTSTUDY = 0; ALLEEG = []; EEG=[]; CURRENTSET=[];
close all
clear EEG ALLEEG ALLCOM LASTCOM PLUGINLIST STUDY
eeglab
pause(5)
end

%% Visual inspection, remove bad channels
for ii = 1:length(subjects)
subject_code = subjects{ii};

```

```

disp(['Current set: ' subject_code]);
channels2reject = channelRejection{ii,:};
EEG = pop_loadset('filename',[subject_code
    '_testNijmegen_continuous_merged.set'],'filepath',pwd);
EEG = pop_saveset(EEG, 'savemode', 'resave');
[ALLEEG EEG] = eeg_store(ALLEEG, EEG, CURRENTSET);
EEG = eeg_checkset(EEG)

% First load the channel locations and labels

channels2reject = sort(channels2reject);
% Load channel labels
load('electrodeLayout132chanLocations.mat');
EEG.chanlocs = chanLoc;
EEG = eeg_checkset(EEG);
% remove channels
EEG = pop_select( EEG,'nochannel',channels2reject);
disp(['Channels removed:' subject_code]);
EEG = eeg_checkset(EEG);
EEG = pop_saveset( EEG, 'savemode', 'resave');
[ALLEEG EEG] = eeg_store(ALLEEG, EEG, CURRENTSET);

% re-reference after removing bad channels
EEG = eeg_checkset( EEG );
EEG = pop_reref( EEG, []);
[ALLEEG EEG CURRENTSET] = eeg_store(ALLEEG, EEG, CURRENTSET);
EEG = eeg_checkset( EEG );
disp(' CAR recomputed!')
EEG = pop_saveset(EEG, 'savemode', 'resave');

% % If used from OSX, load the dataset here by:
% EEG = pop_loadset('filename',[subject_code
    '_testNijmegen_continuous_merged.set'],'filepath',pwd);
% EEG = pop_saveset(EEG, 'savemode', 'resave');
% [ALLEEG EEG] = eeg_store(ALLEEG, EEG, CURRENTSET);
% EEG = eeg_checkset(EEG);

% Save under new name
% Create 0.5 second epochs
EEG = eeg_regepochs(EEG, 0.5, [0 0.5], NaN);
EEG = eeg_checkset(EEG);
[ALLEEG EEG] = eeg_store(ALLEEG, EEG, CURRENTSET);
EEG = eeg_checkset(EEG);
% Save file as '<subject_code>_testNijmegen_rej_epoched.set'
EEG = pop_saveset( EEG, 'filename',[ subject_code '_testNijmegen_rej_epoched.set'], ...
    'filepath',pwd);
EEG = eeg_checkset(EEG);
[ALLEEG EEG] = eeg_store(ALLEEG, EEG, CURRENTSET);

%% RUN BINICA
tic
disp(['BinICA starts now for subject ' subject_code]);
EEG = eeg_checkset(EEG);
[EEG.icaweights,EEG.icasphere] = binica(EEG.data, 'extended', 1, 'maxsteps', 2000);
disp(['BinICA ended at t=' num2str(toc)])
[ALLEEG EEG] = eeg_store(ALLEEG, EEG, CURRENTSET);

% save

```

```

EEG = eeg_checkset( EEG );
EEG = pop_saveset( EEG, 'savemode','resave');
% First ica set is contained in
% '<subject_code>_testNijmegen_rej_epoched.set'
[ALLEEG EEG] = eeg_store(ALLEEG, EEG, CURRENTSET);

%% Run automatic rejection here to prepare for AMICA
% Automatic epoch rejection based on components
tic
EEG = pop_autorej(EEG, 'nogui','on','icacomps',[1:size(EEG.data,1)],'startprob',6);
disp(['Automatic rejection ended at t=' num2str(toc)]);
[ALLEEG EEG CURRENTSET] = eeg_store(ALLEEG, EEG, CURRENTSET);
EEG = eeg_checkset(EEG);

% Save pruned dataset
EEG = pop_saveset(EEG, 'savemode', 'resave');
[ALLEEG EEG] = eeg_store(ALLEEG, EEG, CURRENTSET);
EEG = eeg_checkset(EEG);

pause(2)
STUDY = []; CURRENTSTUDY = 0; ALLEEG = []; EEG=[]; CURRENTSET=[];
close all
clear EEG ALLEEG ALLCOM LASTCOM PLUGINLIST STUDY
eeglab
pause(2)

% perform additional ica
% AMICA
tic
[ EEG.icaweights, EEG.icasphere, mods ] = runamica12( EEG.data(:,,:), 'num_chans',
    size(EEG.data,1)); % DO NOT INCLUDE EMG CHANNELS IN AMICA
disp(['AMICA ended at t=' num2str(toc)]);
[ALLEEG EEG] = eeg_store(ALLEEG, EEG, CURRENTSET);

% EEG = pop_saveset( EEG, 'savemode','resave');
EEG = pop_saveset(EEG, 'filename',[subject_code '_testNijmegen_AMICA.set'], 'filepath', pwd);
[ALLEEG EEG] = eeg_store(ALLEEG, EEG, CURRENTSET);
EEG = eeg_checkset( EEG );
eeglab redraw

%% Reload the merged set and copy ica weights to the continuous data

EEG = pop_loadset('filename',[subject_code
    '_testNijmegen_continuous_merged.set'],'filepath',pwd);
[ALLEEG EEG] = eeg_store(ALLEEG, EEG, CURRENTSET);
EEG = eeg_checkset( EEG );
eeglab redraw

%% load ica set
EEG = pop_loadset('filename',[ subject_code '_testNijmegen_AMICA.set'], ...
'filepath',pwd);
[ALLEEG, EEG, CURRENTSET] = eeg_store( ALLEEG, EEG, 0 );
[ALLEEG EEG CURRENTSET] = pop_newset(ALLEEG, EEG, 2,'retrieve',1,'study',0);
EEG = eeg_checkset( EEG );

EEG = pop_editset(EEG, 'icachansind', ['ALLEEG(' num2str(2) ').icachansind'], ...
'icaweights', ['ALLEEG(' num2str(2) ').icaweights'], ...

```

```
'icasphere', ['ALLEEG(' num2str(2) ').icasphere']);
[ALLEEG EEG] = eeg_store(ALLEEG, EEG, CURRENTSET);
EEG = eeg_checkset( EEG );

EEG = pop_saveset( EEG, 'filename', [subject_code
    '_testNijmegen_continuous_merged.set'], 'filepath', pwd);
[ALLEEG EEG] = eeg_store(ALLEEG, EEG, CURRENTSET);

%% Create condition sets
trigLabel = {'NR', 'NS'};
trigClass = {20, 10};

for k=1:length(trigClass)
EEG = eeg_checkset( EEG );
EEG = pop_epoch( EEG, { num2str(trigClass{k}) }, [-5 5], 'newname', trigLabel{k},
    'epochinfo', 'yes');
[ALLEEG EEG CURRENTSET] = pop_newset(ALLEEG, EEG, 1, 'savenew', ...
    [pwd '/' subject_code '_balance_ICA_' trigLabel{k} '.set'], 'gui', 'off');
EEG = eeg_checkset( EEG );
[ALLEEG EEG CURRENTSET] = pop_newset(ALLEEG, EEG, 2+k, 'retrieve', 1, 'study', 0);
end

eeglab redraw
end
```

C.2. STUDY ANALYSIS

```

%% For all datasets, open the NS version, copy the dipfit data to the NR
%% dataset and save the NR set in the same folder
clear variables
close all
clc

% General
data_path = pwd;
% subject ID's
% subjects = {'as','bl','ch','fb','jj','js','jj','ls','lsv','sl','wc'};
subjects = {'bl','lsv'};

for i = 1:length(subjects)
eeglab
data_path = pwd;
%   subjects = {'as','bl','ch','fb','jj','js','jj','ls','lsv','sl','wc'};
subjects = {'bl','lsv'};
path = [data_path '\ ' subjects{i} '\'];
subject_code = subjects{i};

% open the NS dataset which contains the DIPFIT data
EEG = pop_loadset('filename',[subject_code '_balance_ICA_NS.set'],'filepath',path);
EEG = eeg_checkset(EEG);
[ALLEEG, EEG, CURRENTSET] = eeg_store(ALLEEG, EEG, 0);

EEG = pop_loadset('filename',[subject_code '_balance_ICA_NR.set'],'filepath',path);
EEG = eeg_checkset(EEG);
[ALLEEG, EEG, CURRENTSET] = eeg_store(ALLEEG, EEG, 0);
eeglab redraw

% copy the dipfit data from NS dataset to NR dataset
EEG.dipfit = ALLEEG(1).dipfit;
EEG = eeg_checkset(EEG);
EEG = pop_saveset( EEG, 'filename',[ subject_code '_balance_ICA_NR.set'], 'filepath',path);
clear variables
close all

end

%% STUDY PROCEDURE %%
% Only right-footers
% First find the components that have a RV < 10%
% Second, look within these components for bad trials
% Third; remove bad components and bad trials
% Resave the dataset

% Component indeces with RV < 10%
as = [3 4 5 7 8 9 11 12 13 16 20 31 34 38 47 49 62];
bl = [2 3 5 6 8 10 13 18 20];
jj = [2 3 4 5 6 7 8 10 13 15 17 19 20 21 22 23 25 26 27 28 31 37 38 39 41 43 62];
js = [1 2 3 4 17 23 28 41 51 60 62];
ls = [7 9 10 11 24 26 34 35 47 122];
lsv = [4 7 9 11 12 13 14 18 20 21 24 28 31];
sl = [2 4 7 8 9 10 11 12 13 16 17 26 31 38 39 63];
wc = [2 4 5 7 8 9 12];

```

```

% Components that remain after visual inspection of previous list:
as = [3 4 5 7 8 9 11 12 13 16 20 31 34 38 47 49 62];
bl = [2 3 5 6 10 13 18 20];
jj = [2 3 4 5 6 7 8 10 13 15 17 19 20 21 22 23 25 26 27 28 31 37 38 39 41 43 62];
js = [1 2 3 4 17 23 28 41 51 60 62];
ls = [7 9 10 11 24 26 34 35 47 122];
lsv = [4 7 9 11 12 13 14 18 20 21 24 28 31];
sl = [2 4 7 8 9 10 11 12 13 16 17 26 31 38 39 63];
wc = [2 4 5 7 8 9 12];

% Adjust STUDY contents (STUDY struct contains errors)
setindex = [2 4 6 8 10 12 14 16; 1 3 5 7 9 11 13 15];
STUDY.setind = setindex;
% component indexes saved as compIndex;
compIndex = load('compIndex.mat');
STUDY.cluster.sets = compIndex;
STUDY.cluster.comps = [as bl jj js ls lsv sl wc];

% Calculate cluster centroids
[STUDY, centroid] = std_centroid(STUDY, ALLEEG, cluster, 'dipole');

% Plot all centroids with a different color
figure
colors{1,1} = [1 1 1];           % White
colors{2,1} = [1 1 0];           % Yellow
colors{3,1} = [1 0 1];           % Fuchsia
colors{4,1} = [1 0 0];           % Red
colors{5,1} = [0 1 1];           % Aqua
colors{6,1} = [0 1 0];           % Lime
colors{7,1} = [0 0 1];           % Blue[
colors{8,1} = [0 0 0];           % Black

viewpts = [0 0 1; 0 -1 0; 1 0 0];
figure
% Plot dipole clusters
std_dipoleclusters(STUDY,ALLEEG,'clusters',[3:8],'rowcolplace',[1 3 1],'centroid','off')
%% Plot results of cluster 3 to 8
% Show average scalp map - frequency spectrum (one plot) and ersp (with
% significant values)
subject_codes = {'as','bl','ch','fb','jj','js','ls','lsv','sl','wc'};

% Get number of clusters
numClust = size(STUDY.cluster,2);
plotClust = 3;

% Study analysis
timeRange = [-5000, 5000]; % change as desired
freqRange = [2, 40]; % change as desired
dbLim = 5; % change as desired
dbRange = [-dbLim dbLim];
pvalue = 0.01; % change as desired
baseLine = [-1000 2500];

data_path = 'C:\Users\Joris\Dropbox\2014_2015\Afstuderen\EEG\EEG_data\';
% different statistical parameters
STUDY = pop_statparams(STUDY,
    'condstats','on','alpha',0.01,'statistics','perm','mcorrect','fdr');
STUDY = pop_statparams(STUDY,
    'condstats','on','alpha',pvalue,'statistics','param','mcorrect','none');

```

```

%% ERP
timeRange = [-1000 1500];
% parameters
STUDY = pop_erpparams(STUDY,'timerange',timeRange,'filter',20); % set timerange
pvalue = 0.05;
STUDY = pop_statparams(STUDY,
    'condstats','on','alpha',pvalue,'statistics','perm','mcorrect','fdr');

% Run for all clusters
for i = 3:8
[STUDY, erpdata, erptimes, pgroup, pcond, pinter] = ...
std_erplot(STUDY,ALLEEG,'clusters',i,'noplot','on');
maskedImage = erpdata{2} - erpdata{1}; % NS - NR;
datamat = {erpdata{1}; erpdata{2}}; maskedImage;
datamat = {erpdata{1}; erpdata{2}};
std_plotcurve(erptimes,datamat,'datatype','erp','threshold',pvalue,'condstats',pcond,'plotmode','condensed','title',
    num2str(i) ' p<' num2str(pvalue)],['ERP:IC' num2str(i)],['ERP:IC'
    num2str(i)]},'plotconditions','together','legend',{'Step (NR)','No Step (NS)'});
% Print-friendly figure
fig = gcf;
fig.PaperUnits = 'points';
fig.PaperPosition = [0 0 600/1.5 300/1.5];
fig.PaperPositionMode = 'manual';
% print(gcf,'-dpng',[pwd '\Figures\Cluster_RV10\Cluster_' num2str(i) '_ERP']);
% close(gcf)
end

%% ERSP
% Parameters
pvalue = NaN;
STUDY = pop_statparams(STUDY,
    'condstats','on','alpha',pvalue,'statistics','perm','mcorrect','fdr');
freqRange = [2 150];
timeRange = [-1000 1500];
STUDY = pop_erspparams(STUDY,'timerange',timeRange,'freqRange',freqRange);
% Run for all clusters
for i = 3:8
[STUDY, erspdata, ersptimes, erspfreqs, pgroup, pcond, pinter] = ...
std_erspplot(STUDY,ALLEEG,'clusters',i,'noplot','on', ...
'ersplim',dbRange,'freqrange',freqRange);

meanERSPcond1 = mean(erspdata{1},3);
meanERSPcond2 = mean(erspdata{2},3);
caption = sprintf(['Average ERSP ' STUDY.cluster(i).name '\n NR']);
datamat = {erspdata{1}; erspdata{2}};
std_plottf(ersptimes, erspfreqs, datamat,'condstats',pcond, ...
'ersplim',dbRange,'threshold',pvalue,'titles',{'[STUDY.cluster(i).name ': NR'] ; ...
[STUDY.cluster(i).name ': NS']; 'Condition p-values'});
% Print-friendly figure
fig = gcf;
fig.PaperUnits = 'points';
fig.PaperPosition = [0 0 1000 300];
fig.PaperPositionMode = 'manual';
% print(gcf,'-dpng',[pwd '\Figures\Cluster_RV10\Cluster_' num2str(i) '_ERSP']);
% close(gcf)
clear maskedImage
end

%% Power spectrum
pvalue = 0.05;

```

```

STUDY = pop_statparams(STUDY,
    'condstats','on','alpha',pvalue,'statistics','perm','mcorrect','fdr');
STUDY = pop_specparams(STUDY,'timerange',timeRange,'freqrange',[2 40]);
% Run for all clusters
for i = 3:8
[STUDY, specdata, specfreqs, pgroup, pcond, pinter] = ...
std_specplot(STUDY,ALLEEG,'clusters',i,'noplot','on');
datamat = {specdata{1};
specdata{2};
};
std_plotcurve(specfreqs,datamat,'datatype','spec','threshold',pvalue,'condstats',pcond,'plotmode','condensed',
    'Spectrum:Clust' num2str(i) ' p<'
    num2str(pvalue)]},'plotconditions','together','legend',{'NR','NS'});
% Print-friendly figure
fig = gcf;
fig.PaperUnits = 'points';
fig.PaperPosition = [0 0 300 300];
fig.PaperPositionMode = 'manual';
print(gcf,'-dpng',[pwd '\Figures\Cluster_RV10\Cluster_' num2str(i) '_SPEC']);
close(fig);
end

%% Plot Dipoles
viewp = [1 0 0];
% viewp = [0 -1 0];
for i = 3:8
[STUDY] = std_dipplot(STUDY,ALLEEG, 'clusters', i, 'mode', 'together', 'figure', 'on');
fig = gcf;
fig.PaperUnits = 'points';
fig.PaperPosition = [0 0 1000/3 300];
fig.PaperPositionMode = 'manual';
print(gcf,'-dpng',[pwd '\Figures\Cluster_RV10\Cluster_' num2str(i) '_DIPF_100']);
close(gcf)
end

%% Retrieve trial numbers
% Find how many trials are included per cluster
% First get the set numbers
for i = 3:9
NRtrials = [];
NStrials = [];
setindeces = STUDY.cluster(i).sets;
numcomps = length(setindeces); % number of components
numsubj = unique(STUDY.cluster(i).sets); % find number of subjects
numsubj = length(numsubj)/2; % each subject has 2 datasets
for ii = 1:size(setindeces,2);
% find number of trials for both conditions per subject
nrtrials = size(ALLEEG(setindeces(2,ii)).epoch,2);
nstrials = size(ALLEEG(setindeces(1,ii)).epoch,2);
% store trial numbers
NRtrials(ii) = nrtrials;
NStrials(ii) = nstrials;
end
% sum all trials per cluster
NRtotal = sum(NRtrials); NStotal = sum(NStrials);
disp(['NR total trials for cluster ' num2str(i) ': ' num2str(NRtotal)]);
disp(['NS total trials for cluster ' num2str(i) ': ' num2str(NStotal)]);
end

```
